における抗微生物薬使用の制限が望まれる．

感染症の増加要因

感染症の増加要因は社会要因，宿主要因および病原体要因に大別される．社会的要因として，都市化による過密，貧困，交通機関の発達による高速移動，国際化や感染症対策の軽視などが寄与している．宿主要因として，感染抵抗力の減弱（人口の老齢化，糖尿病，慢性腎不全，ヒト免疫不全ウイルス感染症／後天性免疫不全症候群，免疫抑制薬／臓器移植や免疫疾患など）が易感染性を招来している．また，病原体要因として，新興病原体や薬剤耐性病原体の出現および病原性の変化などが感染症の増加に関与している．

生物テロリズム

感染症による新たな脅威として，炭疽，痘瘡／天然痘，ペスト，野兎病，ボツリヌス症やウイルス性出血熱は生物テロリズムの可能性や懸念を指摘されていたが，2001年10月，炭疽菌（正確には炭疽菌芽胞）による生物テロリズムが現実となり，アメリカ合衆国で23名の炭疽患者（吸入／肺炭疽：11名，皮膚炭疽：12名）が発生し，肺炭疽患者の5名が死亡した[13,14]．さらに，炭疽菌テロリズムでは，発病者のみならず，芽胞曝露者約1万人にフルオロキノロンなど抗微生物薬による予防内服（60日間）が実施され，炭疽菌テロリズムは甚大な社会不安，混乱や被害を惹起した．すなわち，生物テロリズムの観点からも感染症危機管理体制の確立は急務であり，2007年の感染症法改正で「生物テロ」に関する特定病原体の管理体制を強化している[15]．

施設内（特に，院内）感染

院内感染症は「入院から48時間以降に発症した感染症」と定義されている．感染源は1）人的要因：患者，医療従事者，訪問者，また，2）環境要因：汚染医療器具／機器，食物，水，空気などである．医療の高度化，易感染者（高齢者を含む）の増加，日和見感染や薬剤耐性病原体の増加に伴い，院内感染は重要な課題となっている．院内感染の出現頻度では，1）尿路感染，2）外科的創部感染，3）呼吸器感染，4）菌血症や敗血症が多い．従って，病院は院内で発生した感染症に関し，その発生状況の把握（Hospital epidemiology）に努め，院内感染が疑われる場合，感染源や感染経路を解明することにより，感染の拡大を防止するための迅速な対応が急務となる．

施設内感染対策の基本は，手洗いの励行，清掃など施設内環境整備，施設内感染に正しい知識の啓発である．1996年，アメリカ合衆国疾病管理防疫センター（Centers for Disease Control and Prevention：CDC）は病院内感染防止指針を提唱している．その骨子は2要素，標準的予防措置（Standard precautions）および感染伝播予防措置（Transmission-based precautions）から構成されている[16]．

行政対応

新興・再興感染症の台頭／出現，医学・医療の進歩，公衆衛生水準の向上，人権尊重と行政の透明化，事前対応型行政，国際化への対応／国際協力の推進，発生動向調査の推進および動物由来感染症対策の充実を指向し，1999年4月01日から「感染症の予防および感染症の患者に対する医療に関する法律」（法律第114号）が施行されている．従来の「伝染病予防法」，「性病予防法」および「エイズ予防法」を廃止・統合し，新時代に即応した感染症対策を推進している．さらに，2007年4月，「結核予防法」統廃合，生物テロに関する特定病原体の管理強化や感染症の分類の見直しを主旨とする感染症法の改正が施行された[11,15]．

おわりに

感染症は現在でも，人類に甚大な健康被害を提供し，さらに，新興・再興感染症や薬剤耐性病原体感染症は世界的に増加しており，直近においても，新型インフルエンザ出現など，油断できない状況にある．感染症対策は感染源，感染経路および感受性宿主対策を基盤とし，1）教育・環境・行政など社会基盤整備，2）抗微生物化学療法，3）免疫介入療法，4）併用療法（抗微生物化学および免疫介入療法）が推進されている．しかし，感染症対策の基本は予防であり，予防における最も効果的，かつ，科学的戦略は宿主を治療標的，かつ，有効活用した免疫介入療法：予防接種／ワクチンであることは過去，現在，将来共に不変であろう[17,18]．事実，人類が根絶した唯一の疾患は痘瘡／天然痘であり，その勝利の

原動力はワクチンであった．微生物を用いた古典的ワクチン，非細胞性成分ワクチン，細胞培養ワクチン，遺伝子ワクチンなどの新規ワクチン，感染症に対する遺伝子治療などが登場するであろう．加えて，肝細胞癌：B型肝炎ウイルスや子宮頸癌：ヒト乳頭ウイルスではワクチン接種が実施されており，今後，これら病原体感染による悪性腫瘍の減少が期待される．

野生型ポリオ根絶，次いで，麻疹，百日咳，ジフテリア，結核の制圧や根絶に人類は邁進するであろう．しかし，微生物界は新興病原体や薬剤耐性微生物を産出して，人間社会に侵入し，健康に対する脅威を提供することが反復されるだろう．さらに，腸管出血性大腸菌感染症，メチシリン耐性ブドウ球菌感染症や結核などの集団・病院を含めた施設内感染，また，生物テロも脅威であり，感染症危機管理体制の確立は急務の課題である．

21世紀の世界や人類は感染症と戦い，制圧／根絶，あるいは共存を指向した新しい道を模索することになるが，この過程には多くの困難や障害が待ち受けていることだろう．教育・環境・行政・社会基盤整備に加えて，人類の叡智が感染症を克服することを，そして，健康被害を減少させることを期待している．

謝辞　本稿は，厚生労働省　厚生労働科学研究費補助金（新型インフルエンザ等新興・再興感染症研究事業，医薬品・医療機器等レギュラトリーサイエンス総合研究事業，政策創薬総合研究事業），文部科学省　科学研究費補助金，科学技術振興調整費，日米医学協力研究会結核・ハンセン病専門部会により支援された．

文　献

1) World Health Organization. The World Health Report. http://www.who.int/whr/en/（参照 2010-04-21）
2) Time: Global Health Summit. http://www.time.com/time/2005/globalhealth/（参照 2010-04-21）
3) World Health Organization. Global burden of disease, http://www.who.int/healthinfo/global_burden_disease/en/（参照 2010-04-21）
4) Morens, DM, GK Folkers, and AS Fauci: The challenge of emerging and re-emerging infectious diseases. *Nature* 430：242-249, 2004. http://www.nature.com/nature/journal/v430/n6996/full/nature02759.html（参照 2010-04-21）
5) World Health Organization. Pandemic (H1N1) 2009. http://www.who.int/csr/disease/swineflu/en/index.html（参照 2010-04-21）
6) Centers for Disease Control and Prevention. Seasonal influenza. http://www.cdc.gov/flu/keyfacts.htm（参照 2010-04-21）
7) 国立感染症研究所感染症情報センター：パンデミック（H1N1）2009. http://idsc.nih.go.jp/disease/swine_influenza/index.html（参照 2010-04-21）
8) 厚生労働省．健康局結核感染症課：平成20年結核登録者情報調査年報集計結果（概況）．http://www.mhlw.go.jp/bunya/kenkou/kekkaku-kansenshou03/08.html（参照 2010-04-21）
9) Stop TB Partnership. http://www.stoptb.org/（参照 2010-04-21）
10) エイズ予防情報ネット．http://api-net.jfap.or.jp/（参照 2010-04-21）
11) 厚生労働省．健康局結核感染症課：感染症情報．http://www.mhlw.go.jp/bunya/kenkou/kekkaku-kansenshou.html（参照 2010-04-21）
12) 厚生労働省．健康局結核感染症課．感染症法に基づく医師および獣医師の届出について．http://www.mhlw.go.jp/bunya/kenkou/kekkaku-kansenshou11/01.html（参照 2010-04-21）
13) Centers for Disease Control and Prevention. Public health emergency preparedness and response, http://www.bt.cdc.gov/, http://emergency.cdc.gov/bioterrorism/（参照 2010-04-21）
14) Centers for Disease Control and Prevention. Anthrax. http://emergency.cdc.gov/agent/anthrax/（参照 2010-04-21）
15) 厚生労働省．健康局結核感染症課：感染症法に基づく特定病原体等の管理規制について．http://www.mhlw.go.jp/bunya/kenkou/kekkaku-kansenshou17/03.html（参照 2010-04-21）
16) Centers for Disease Control and Prevention. Infection Control Healthcare Settings. http://www.cdc.gov/ncidod/dhqp/index.html（参照 2010-04-21）
17) Centers for Disease Control and Prevention. Vaccines and Immunizations. http://www.cdc.gov/vaccines/（参照 2010-04-21）
18) 国立感染症研究所感染症情報センター：予防接種情報．http://idsc.nih.go.jp/vaccine/vaccine-j.html（参照 2010-04-21）

MAJOR ARTICLE

Analysis of Drug-Resistant Strains of *Mycobacterium leprae* in an Endemic Area of Vietnam

Masanori Kai,[1] Nhu Ha Nguyen Phuc,[2] Hoang An Nguyen,[2] Thi Hoang Bich Diu Pham,[2] Khanh Hoa Nguyen,[2] Yuji Miyamoto,[1] Yumi Maeda,[1] Yasuo Fukutomi,[1] Noboru Nakata,[1] Masanori Matsuoka,[1] Masahiko Makino,[1] and Thanh Tan Nguyen[2]

[1]Department of Mycobacteriology, Leprosy Research Center, National Institute of Infectious Diseases, Higashimurayama, Tokyo, Japan; and [2]Quyhoa National Leprosy and Dermato-Venereology Hospital, Quynhon City, Binhdinh, Vietnam

(See brief report by Ramien and Wong, e133–e135.)

Background. Multidrug therapy has effectively reduced the number of leprosy cases in the world. However, the rate of reduction has decelerated over the years, giving early detection of *Mycobacterium leprae* and epidemiological study of relapse renewed relevance in attempts to eliminate the disease.

Methods. A molecular epidemiological survey for drug-resistant *M. leprae* was conducted in the central and highland regions of Vietnam. A total of 423 samples taken from patients, including 83 patients with new cases, 321 patients receiving treatment, and 19 patients with relapse, were studied for detection of *M. leprae* with mutations relating to drug resistance by sequencing the drug resistance determining region of the *folP1*, *rpoB*, and *gyrA* genes, which are responsible for dapsone, rifampicin, and ofloxacin resistance, respectively.

Results. Nineteen mutations were found in the *folP1* gene samples, and no mutations relating to drug resistance were found in either the *rpoB* or *gyrA* genes. Samples from patients with relapse showed *folP1* mutation rates as high as 57%, and the mutation rates in samples from new and recent cases were <10%. Patients with relapse who had histories of treatment with dapsone monotherapy showed high mutation rates (78%), compared with patients with relapse who had previously only received multidrug therapy (33%).

Conclusions. Our study indicated high rates of dapsone resistance in patients with relapse, compared with patients with new and recent cases of leprosy. Moreover, it was observed that many of the patients with relapse who had dapsone-resistant mutations had histories of treatment with dapsone monotherapy.

Leprosy is a chronic infectious disease caused by infection with *Mycobacterium leprae*. The present strategy for leprosy control is based on the multidrug therapy (MDT), recommended by the World Health Organization (WHO) [1], which has successfully reduced the number of leprosy cases in the world. However, transition in the number of registered cases and new cases amounting to ~210,000 and ~250,000, respectively, has almost come to a standstill [2]. Drug-resistant strains were first found in 1964, 1976, and 1997 [3–5]. MDT was designed to prevent the emergence and spread of drug-resistant strains. However, a strain showing resistance to both dapsone and rifampicin was reported in 1993 [6], and at present, there are further reports indicating the emergence of *M. leprae* strains resistant to multiple drugs [5, 7]. At present, the rapid detection and control of such drug-resistant strains is essential in countries approaching leprosy elimination levels, such as Vietnam.

MDT has been quite successful in Vietnam, and elimination of leprosy (prevalence rate, < 1/10,000 population) was achieved on the national level in 1995 [8]. The prevalence rate per 10,000 population in 2006

Received 28 August 2010; accepted 7 December 2010.

Correspondence: Masanori Kai, MD, Department of Mycobacteriology, Leprosy Research Center, National Institute of Infectious Diseases, 4-2-1 Aoba-cho, Higashimurayama, Tokyo 189-0002, Japan (mkai@nih.go.jp).

Clinical Infectious Diseases 2011;52(5):e127–e132
© The Author 2011. Published by Oxford University Press on behalf of the Infectious Diseases Society of America. All rights reserved. For Permissions, please e-mail:journals.permissions@oup.com.
1058-4838/2011/525-0001$37.00
DOI: 10.1093/cid/ciq217

Downloaded from cid.oxfordjournals.org at National Institute of Infectious Diseases, Library on February 3, 2011

was .07 [8, 9]. However, the majority of patients with leprosy are found in the central and highland regions of Vietnam [10], consisting of 11 provinces, including 4 provinces in the highland region and 7 provinces in the delta region. In 2005, the number of patients with leprosy was 236, spread through 4 provinces of the highland region; the prevalence rate of newly detected cases was 3.5 cases/10,000 population, although the overall prevalence rate was .25 cases/100,000 population on the national level. The rate of newly detected cases in the 7 delta region provinces was 1.38 cases/10,000 population [8, 9]. These cases not only present the danger of being possible infectious sources for leprosy but also harbor the risk of developing into relapse cases. However, little is known regarding the effects of drug-resistant *M. leprae* in patients with leprosy, especially in cases of relapse.

Therefore, in the present study, molecular epidemiological studies on drug-resistant strains were conducted in 11 provinces primarily in the central and highland regions that represent the areas where leprosy is endemic in Vietnam.

MATERIALS AND METHODS

Sensitivity of Polymerase Chain Reaction

The number of bacilli isolated from nude mice footpads was counted using the method described by Shepard et al [11]. Serial 10-fold dilutions of the enumerated *M. leprae* bacilli were used for polymerase chain reaction (PCR) in our study.

Clinical Specimens

Samples (from slit-skin smears or punch biopsies) were taken from patients with leprosy after receipt of informed consent in primarily the central and highland regions of Vietnam (including 11 provinces: Danang, Quangnam, Quangngai, Binhdinh, Phuyen, Khanhhoa, Ninhthuan, Kontum, Gialai, Daknong, and Daklak), and the samples were classified as new (before starting MDT), recent (receiving MDT), and relapse cases. Relapse was defined as development of new skin lesions after completion of MDT and increase in bacterial index by >2 log units in any lesion.

The total of 423 samples included those from 83 patients with new cases, 321 patients with recent cases (receiving treatment), and 19 patients with relapse (collection period: March 2004–August 2009). Among 16 patients with relapse who had positive results of *M. leprae*–specific PCR, 9 cases were determined to be relapse after dapsone monotherapy (7–20 years), 3 as relapse after complete MDT, 2 as second relapse (the first after dapsone monotherapy and the second after MDT), and 2 as relapse after ofloxacin treatment. Samples were obtained from the skin lesions of patients (smear on blade or biopsy soaked in 1 mL of 70% ethanol at room temperature in the field, before being sent to Quyhoa National Leprosy & Dermato-Venereology Hospital laboratory).

DNA Extraction, Nested PCR, and Sequencing

M. leprae templates from both dilutions of *M. leprae* bacilli and slit-skin smears were prepared by treatment with lysis buffer at 60°C overnight, as described elsewhere [12]. Nested PCR amplification of the RLEP regions of *M. leprae* was performed under conditions described elsewhere with minor modifications, using the primers listed in Table 1 [13]. In brief, PCR amplification using special reagents (20 mM Tris-HCl [pH, 7.5], 8 mM magnesium chloride, 7.5 mM DTT, 2.5 mg BSA, 150 μM deoxynucleotides, 1.5 mM magnesium sulphate, and 2.5 units KOD-plus-Ver.2 DNA polymerase [Toyobo]) was performed using sample DNA as templates. Both first and second PCR conditions were as follows; strand separation at 94°C for 4 min, denaturing at 94°C for 40 s, annealing at 55°C for 1 min, and extension at 72°C for 20 s plus 1-s increment per cycle for 25 cycles. Products from the first PCR (0.5 uL) were used as templates in the second PCR. The nested PCR for DRDR was performed using the primer pairs listed in Table 1. Mutations were measured on the *folP1* gene for dapsone [14], the *rpoB* gene for rifampicin, and the *gyrA* gene for ofloxacin [15, 16]. Nested PCR conditions for drug resistance were different from that for RLEP-nested PCR. In brief, PCR amplification using standard reagents (10 mM Tris-HCl [pH, 8.3], 2 mM magnesium chloride, 250 μM dNTPs, and 2.5 units TaKaRa Ex Taq DNA polymerase [Takara shuzo]) was performed using sample genomic DNA as templates. The primer pairs used to amplify the specific drug-resistant genes are shown in Table 1. The reaction condition was 30 s at 94°C, 30 s at 60°C, and 1 min at 72°C for 35 cycles.

The amplicons were visualized by agarose gel electrophoresis, and DNA was recovered from the gel using Mini-Elute gel extraction kits (Qiagen). The recovered DNA molecules were sequenced using the ABI Prism BigDye Terminator Cycle Sequencing kit (Perkin-Elmer Applied Biosystems) and run on an ABI Prism 3130 Genetic Analyzer (Applied Biosystems). The sequence data were analyzed by DNA analysis program Genetyx-MAC, version 15 (GENETYX), and were compared with those in the GenBank database.

RESULTS

PCR Sensitivity

Serial dilutions of the bacilli of 1×10^8–1×10^0 were prepared to determine PCR sensitivities. Genomic DNAs were extracted from the diluents with use of methods described under Materials and Methods [11]. The previously reported RLEP-nested PCR (named RLEP-L) was capable of detecting 1×10^2 bacilli in samples (Figure 1a) [13]. The newly designed RLEP-nested PCR, using K1 and K2 primers for the first PCR and LP1 and LP2 primers for the second PCR (named RLEP-K), is capable of detecting comparable counts of bacilli (Figure 1b), and RLEP-K

Downloaded from cid.oxfordjournals.org at National Institute of Infectious Diseases, Library on February 3, 2011

Table 1. Sequences of Primers Used in this Study

Name	Usage	Gene	Sequence, 5′→3′	Reference	Size, bp
K1	First PCR (F)	RLEP	CGTGGGTGTGAGGATAGTTGT-	Present study	268
K2	First PCR (R)	RLEP	GATCATCGATGCACTGTTCACT-	Present study	
LP1	First or second PCR (F)	RLEP	TGCATGTCATGGCCTTGAGG-	13	129
LP2	First or second PCR (R)	RLEP	CACCGATACCAGCGGCAGAA	13	
LP3	Second PCR (F)	RLEP	TGAGGTGTCGGCGTGGTC	13	99
LP4	Second PCR(R)	RLEP	CAGAAATGGTGCAAGGGA	13	
F1	Second PCR (F)	*folP1*	GCAGGTTATTGGGGTTTTGA	Present study	312
F2	First PCR(R)	*folP1*	CCACCAGACACATCGTTGAC	Present study	
F3	Second PCR (F)	*folP1*	CTTGATCCTGACGATGCTGT	Present study	245
F4	Second PCR(R)	*folP1*	ACATCGTTGACGATCCGTG	Present study	
F5	Sequencing primer (F)	*folP1*	ATCCTGACGATGCTGTCCA	Present study	–
F4	Sequencing primer (R)	*folP1*	ACATCGTTGACGATCCGTG	Present study	–
R1	First PCR (F)	*rpoB*	CAGACGCTGATCAATATCCGT	Present study	358
R2	First PCR (R)	*rpoB*	CAGCGGTCAAGTATTCGATC	Present study	
R3	Second PCR (F)	*rpoB*	CAATATCCGTCCGGTGGTC	Present study	337
R4	Second PCR (R)	*rpoB*	GTATTCGATCTCGTCGCTGA	Present study	
R5	Sequencing primer (F)	*rpoB*	ACGCTGATCAATATCCGTCC	Present study	–
R6	Sequencing primer (R)	*rpoB*	CGACAA TGAACCGATCAGAC	Present study	–
G1	First PCR (F)	*gyrA*	ACGCGATGAGTGTGATTGTGG	Present study	336
G2	First PCR (R)	*gyrA*	TCCCAAATAGCAACCTCACC	Present study	
G3	Second PCR(F)	*gyrA*	GATGGTCTCAAACCGGTACA	Present study	291
G4	Second PCR (R)	*gyrA*	CCCAAATAGCAACCTCACCA	Present study	
G3	Sequencing primer (F)	*gyrA*	GATGGTCTCAAACCGGTACA	Present study	–
G4	Sequencing primer (R)	*gyrA*	CCCAAATAGCAACCTCACCA	Present study	–

products are visualized more clearly with less smear bands. Therefore, the new RLEP-K system was used for detection in further experimentation with use of clinical samples.

Using DNAs extracted from the serial dilutions of *M. leprae*, we determined the sensitivity of the nested PCR for DRDRs. The limit of amplification by PCR was 1×10^3–1×10^4 bacilli (Figure 1 c–e).

RLEP-nested PCR for Clinical Samples

The PCR methods were applied on 423 clinical samples collected from areas of endemicity in Vietnam. First, we tested RLEP-K for detection of *M. leprae* after extraction of DNA from smear samples. Positive bands were obtained by gel electrophoresis using RLEP-K on 290 samples. The positivity rate was 69%. The patients supplying the 290 samples were divided into 3 categories: new, relapse, and recent cases. Positive rates of RLEP-K by category were 75%, 84%, and 66%, respectively (Table 2).

Mutations in Clinical Samples

Samples positive by RLEP-nested PCR were applied for mutation experiments on the DRDRs of *folP1*, *rpoB*, and the *gyrA* gene. Nineteen mutations were found in 187 *folP1* samples, but no mutations related to drug resistance were noted in 163 *rpoB* and 147 *gyrA* gene samples. The mutations detected on *folP1* were as follows: 6 cases of ACC to ATC in codon 53(threonine to isoleucine), 9 cases of CCC to CGC in codon 55 (proline to arginine), and 4 cases of CCC to CTC (proline to leucine). Two new cases, 8 relapse cases, and 9 recent cases had mutations on *folP1*. Mutation rates in the 3 categories were 6.1%, 57%, and 6.4%, respectively (Table 3).

Some missense mutations, of which the association with drug resistance is unknown, were detected in the *rpoB* gene from clinical samples. The mutations were detected in 7 patients at codons 517, 532, and 556. One patient with relapse showed a mutation from CAG (glutamine) to CAT (histidine) at codon 517. One new patient showed 2 mutations at codon 517 from CAG (glutamine) to CAT (histidine) and at codon 532 from GCG (alanine) to TCG (serine). Sequence electropherograms indicated double peaks of a second nucleotide at codon 556 in 3 patients categorized as having recent cases. One peak was G (identical to that of wild-type), and the other peak was T, which changed the amino acid from glycine (GGC) to valine (GTC; data not shown).

The Relation between Treatment and Drug-Resistant Mutations in Patients with Relapse

Patients with relapse were categorized into 4 groups, by treatment history (Table 4). Group 1 comprised those treated with dapsone monotherapy. Group 2 was treated with MDT for 24 months. Group 3 included patients who had received

Downloaded from cid.oxfordjournals.org at National Institute of Infectious Diseases, Library on February 3, 2011

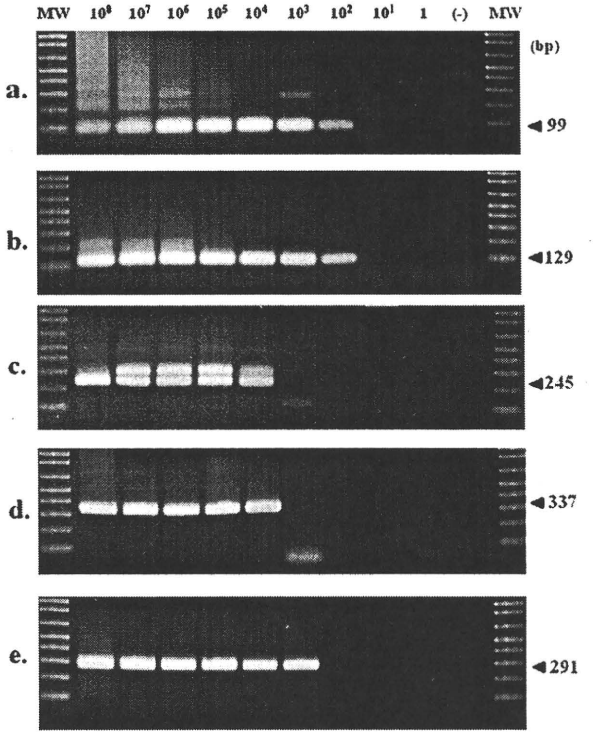

Figure 1. Sensitivity of nested polymerase chain reaction (PCR). The nested PCR products were visualized on 2 % agarose gel. A, RLEP-nested PCR (RLEP-L) using primers, LP1-LP4 (final products size, 99 bp). B, RLEP-nested PCR (RLEP-K) using primers, K1, K2, LP1, and LP2 (final products size, 129bp). C, *folP1*-nested PCR using F1-F4. D, *rpoB*-nested PCR using R1-R4. E, *gyrA*-nested PCR using G1-G4.

a diagnosis of second relapse—once after treatment with dapsone monotherapy and, subsequently, after MDT for 24 months. Group 4 was treated with ofloxacine monotherapy. Eight of the 14 patients with *folP1*-amplified relapse cases (57%) had mutations on the *folP1* gene. Seven (78%) of 9 patients with relapse who were categorized in groups 1 and 3 also had *folP1* mutations. However, 2 patients in group 4 had no mutations on any of the 3 genes.

Monitoring of Mutations in Patients

One hundred seven slit-skin smear samples from 43 patients were taken with consents at different times from each patient for monitoring mutations under treatment. Table 5 shows the difference in mutation results between 5 such patients. The other 38 patients showed no mutation during monitoring. Patients A, B, and C, who had new cases, showed a similar pattern, with no mutation at first testing and mutation in codon 53 on the *folP1* gene during MDT. However, double peaks of T and C in the second base were observed on *folP1* in the 3 patients. Patients D and E, who had relapse cases and finished dapsone monotherapy 20 years earlier, had a mutation on *folP1* in 2005 and no mutation after MDT.

Table 2. Polymerase Chain Reaction Positivity in New, Relapse, and Recent Cases

Case category	No.	RLEP	*folP1*	*rpoB*	*gyrA*
New	83	62 (75%)	33	39	43
Relapse	19	16 (84%)	14	15	13
Recent	321	212 (66%)	140	109	91
Total	423	290 (69%)	187 (64%)	163 (56%)	147 (51%)

DISCUSSION

The most popular PCR method for *M. leprae* detection with high sensitivity and specificity is probably the RLEP-nested PCR method, because the RLEP regions are specific for *M. leprae*, with >28 copies dispersed through the *M. leprae* genome [17]. New primers were designed for the RLEP-nested PCR in our study. This system using the new primers was termed RLEP-K. RLEP-K products appear to be a somewhat sharper and stronger band on agarose gel electrophoresis, compared with that that of previous RLEP-nested PCR (ie, RLEP-L). The RLEP-K detected *M. leprae* in 69% of the Vietnam samples. The remaining 31% of the samples were deduced as being cases either cleared of *M. leprae* by chemotherapy or those having <100 bacilli, which was below the detection limit of RLEP-K. We also designed new primers for amplification and sequencing of DRDR in the drug-resistance related genes *folP1*, *rpoB*, and *gyrA*, which were applied in examining the Vietnam samples. The mutation rates of *folP1* in new and recent cases were 6.1% and 6.4%, respectively. In contrast, the mutation rate in relapse cases was quite high, at 57%. The result indicated a strong correlation between mutation rate and relapse. Two possible reasons were conceived regarding the high positive rate of dapsone resistance in patients with relapse: (1) reinfection by the primary drug-resistant strain (7 of 8 samples indicating relapse were collected in the province in central Vietnam, which had the highest prevalence of leprosy and high rate of relapse (data not shown) and (2) reactivation of dapsone-resistant strains capable of

Table 3. Number of Mutations on *folP1*

Case category	No. of PCR-positive cases	No. of mutations (mutation ratio)	No. of mutation in mutation types
New	33	2 (6.1%)	2 (55th: CCC-CGC)
Relapse	14	8 (57%)	2 (53rd: ACC-ATC)
			3 (55th: CCC-CGC)
			3 (55th: CCC-CTC)
Recent	140	9 (6.4%)	4 (53rd: ACC-ATC)
			4 (55th: CCC-CGC)
			1 (55th: CCC-CTC)

Downloaded from cid.oxfordjournals.org at National Institute of Infectious Diseases, Library on February 3, 2011

Table 4. Mutations Noted in RLEP-Positive Relapse Cases, by Treatment Group

Group	Past treatment	No.	Mutation on *folP1*	Mutation on *rpoB*	Mutation on *gyrA*
1	DDS	7	5	0	0
2	MDT (24 months)	3	1	1[a]	0
3	DDS plus MDT (24 months)	2	2	0	0
4	OFX	2	0	0	0
All	...	14	8	1[a]	0

Abbreviations: DDS (diaminodiphenylsulfone), dapsone monotherapy; MDT,multidrug treatment; OFX, Ofloxacine monotherapy.

[a] Unknown DR mutation

persisting after chemotherapy, discussed below. Although it is still unclear whether the relapses are caused by reinfection by *M. leprae* or by reactivation of persistent *M. leprae*, close correlation between drug resistance and relapse have been recognized in several studies [18, 19].

The proportion of samples showing mutation on the *folP1* gene related to dapsone resistance was 10.2% (19 of 187) in samples from the central and highland regions of Vietnam (Table 3). Comparison with previous reports from South Korea (19.2%) indicates lower rates of relapse in these regions of Vietnam [20].

No mutation was found in the DRDR regions of *rpoB* in all samples. Mutation frequencies of the *rpoB* gene are also very low in other reports. Regarding other areas in Southeast Asia, no cases of rifampicin resistance have been detected in the Philippines, 1 (1.9%) of 54 cases in Myanmar, and 4 (3.3%) of 121 cases in Indonesia. However, in Japan, where the prevalence of leprosy is very low, the reported rate of rifampicin resistance is very high, at 29.5% (26 of 88 cases) [21]. The long-term use of drugs outside the standard MDT regimen in Japanese leprosy cases might have been instrumental in promoting this rifampicin resistance.

As such, no mutations have been found in the DRDR of the *M. leprae rpoB* gene derived from patients with leprosy, including relapse cases in Vietnam. A possible explanation for this could be the success of leprosy control in Vietnam and efficacy of properly administered MDT in which rifampicin—with its bactericidal properties—was effective in suppressing the occurrence of drug-resistant bacilli. In contrast, dapsone (not bactericidal in itself, although capable of suppressing growth), which had previously been used as monotherapy, may have enabled bacteria surviving in the patient receiving treatment to develop mutations, giving them resistance against the drug. Although occurrence of drug-resistant *M. leprae* was kept very low after application of MDT, 7 of 9 samples with drug-resistant mutations had previously been treated by dapsone monotherapy (Table 4). Jing et al [22] reported that patients with multibacillary leprosy who were retreated with MDT after dapsone monotherapy may have lower risk of early relapse while continuing to carry the risk of late relapse. Our observations suggest the possibility that efficacy of MDT may be hampered in some patients by the presence of surviving dapsone-resistant *M. leprae* in their bodies, which could develop into late relapse. Similar observations have been reported, suspecting involvement of the effects of dapsone monotherapy in patients with relapse [23].

There was no mutation in the major sites for drug resistance on the *rpoB* gene. However, we observed mutations at 3 positions, codons 517, 532, and 556, which have not been associated with rifampicin resistance. These mutations in the *rpoB* gene are a finding calling for further clarification.

Table 5. Monitoring of 5 Patients with Multibacillary Leprosy for *folP1* Mutation

Patient	Case category	Date of sample obtainment	Sample site (method of obtainment)	*folP1* mutation
A	New	2006 April 3	Abdomen (biopsy)	None[a]
		2007 January 30	Earlobe (smear)	53rd (ACC→ATC/ACC)
		2007 January 30	Abdomen (smear)	53rd (ACC→ATC/ACC)
B	New	2005 May 31	Earlobe (smear)	None
		2006 March 24	Skin (smear)	None
		2007 November 2	Skin (smear)	53rd (ACC→ATC/ACC)
C	New	2006 July 20	Skin (smear)	None
		2007 January 30	Skin (smear)	53rd (ACC→ATC/ACC)
		2007 January 30	Skin (smear)	53rd (ACC→ATC/ACC)
D	Relapse	2005 November	Earlobe (smear)	55th (CCC→CGC)
		2007 January	Skin (smear)	None
E	Relapse	2007 Jannuary 17	Arm (smear)	None
		2007 January 30	Earlobe (smear)	55th (CCC→CGC)
		2007 January 30	Arm (smear)	None

[a] ACC ATC/ACC indicates double peaks in second base at codon 53.

Downloaded from cid.oxfordjournals.org at National Institute of Infectious Diseases, Library on February 3, 2011

To reveal the possible relation between treatment and gene mutation, some patients with leprosy were monitored for gene mutations in light of drug treatments. The results showed incidence of dapsone-resistant *M. leprae* in patients receiving MDT, suggesting that some of the patients with relapse who were previously treated with dapsone monotherapy might have persistent infections with dapsone-resistant *M. leprae*. Furthermore, samples derived from different sites of lesions in the same patient sometimes showed different results (Table 5). The results suggest that we need to know the relation between the situation of patients with leprosy and drug resistance.

Overall, our study indicated a high ratio of dapsone resistance in patients with relapse, compared with the other patients with leprosy. In contrast, an unexpected outcome of our study was that we were unable to find mutations on the *rpoB* gene in patients with relapse. Moreover, it was shown that many of the patients with relapse who had dapsone-resistant mutations had histories of treatment with dapsone monotherapy. To clarify the relationship between relapse, drug resistance, and dapsone monotherapy, it might be necessary to investigate persistence of drug-resistant *M. leprae* through large-scale surveillance.

Acknowledgments

We thank all medical officers working in the local health centers of the 11 provinces in the central and highland regions of Vietnam for their help in collecting the clinical samples.

Financial support. Thos work was supported by Ministry of Health of Vietnam; Quyhoa National Leprosy & Dermato-Venereology Hospital, Vietnam; Japan Health Sciences Foundation; and a Health Science Research Grant—Research on Emerging and Re-emerging Infectious Diseases, Ministry of Health, Labour and Welfare, Japan.

Potential conflicts of interest. All authors: no conflicts.

References

1. WHO Study Group. Chemotherapy of leprosy for control Programmes. Geneva: Tech Resp Ser, 1982: 675.
2. World Health Organization (WHO). Global leprosy situation. Wkly Epidemiol Rec **2009**; 84:333–40.
3. Rees RJ. Mycobacterial disease in man and animals. Studies on leprosy bacilli in man and animals. Proc R Soc Med **1964:**; 57:482–3.
4. Jacobson RR, Hastings RC. Rifampin-resistant leprosy. Lancet **1976**; 2:1304–5.
5. Cambau E, Perani E, Guillemin I, Jamet P, Ji B. Multidrugresistance to dapsone, rifampicin, and ofloxacin in *Mycobacterium leprae*. Lancet **1997**; 349:103–4.
6. González AB, Maestre JL, Hernández O, et al. Survey for secondary dapsone and rifampicin resistance in Cuba. Lepr Rev **1993**; 64:128–35.
7. Matsuoka M, Kashiwabara Y, Namisato MA. *Mycobacterium leprae* isolate resistant to dapsone, rifampin, ofloxacin and sparfloxacin. Int J Lepr Other Mycobact Dis **2000**; 68:452–5.
8. World Health Organization (WHO). Global leprosy situation. Wkly Epidemiol Rec **2008**; 83:217–24.
9. Bang PD, Suzuki K, Ishii N, Kang TH. Leprosy situation in Vietnam-reduced burden of stigma. Jpn J Lep **2008**; 77:29–36.
10. Quyhoa NDH. Annual report (2004–2009). http://www.quyhoandh.org.vn/quyhoandh/vn/portal/index.jsp. Accessed 29 December 2010.
11. Shepard CC. The experimental disease that follows the injection of human leprosy bacilli into foot-pads of mice. J Exp Med **1960**; 112:445–54.
12. de Wit MY, Faber WR, Krieg SR, et al. Application of a polymerase chain reaction for the detection of *Mycobacterium leprae* in skin tissues. J Clin Microbiol **1991**; 29:906–10.
13. Donoghue HD, Holton J, Spigelman M. PCR primers that can detect low levels of *Mycobacterium leprae* DNA. J Med Microbiol **2001**; 50:177–82.
14. Kai M, Matsuoka M, Nakata N, et al. Diaminodiphenylsulfone resistance of *Mycobacterium leprae* due to mutations in the dihydropteroate synthase gene. FEMS Microbiol Lett **1999**; 177:231–5.
15. Honore N, Cole ST. Molecular basis of rifampin resistance in *Mycobacterium leprae*. Antimicrob Agents Chemother **1993**; 37:414–8.
16. Maeda S, Matsuoka M, Nakata N. Multidrug resistant *Mycobacterium leprae* from patients with leprosy. Antimicrob Agents Chemother **2000**; 45:3635–9.
17. Cole ST, Eiglmeier K, Parkhill J, et al. Massive gene decay in the leprosy bacillus. Nature **2001**; 409:1007–11.
18. Kaimal S, Thappa DM. Relapse in leprosy. Indian J Lepr **2009**; 75:126–35.
19. Lopez-Roa RI, Fafutis-Morris M, Matsuoka M. A drug-resistant leprosy case detected by DNA sequence analysis from a relapsed Mexican leprosy patient. Rev Latinoam Microbiol **2006**; 48:256–9.
20. You EY, Kang TJ, Kim SK, et al. Mutations in genes related to drug resistance in *Mycobacterium leprae* isolates from leprosy patients in Korea. J Infect **2005**; 50:6–11.
21. Matsuoka M, Budiawan T, Aye KS, et al. The frequency of drug resistance mutations in *Mycobacterium leprae* isolates in untreated and relapsed leprosy patients from Myanmar, Indonesia and the Philippines. Lepr Rev **2007**; 78:343–52.
22. Jing Z, Zhang R, Zhou D, Chen J. Twenty five years follow up of MB leprosy patients retreated with a modified MDT regimen after a full course of dapsone mono-therapy. Lepr Rev **2009**; 80:170–6.
23. Chakma JK, Girdhar A, Natrajan M, et al. Two microbiological relapses in a patient with lepromatous leprosy. Lepr Rev **2008**; 79:331–4.

Downloaded from cid.oxfordjournals.org at National Institute of Infectious Diseases, Library on February 3, 2011

LASER WORDS	TRA	tra'1165	B	Dispatch: January 31, 2011	Journal: TRA	CE: G.Priya
	Journal Name	Manuscript No.		Author Received:	No of pages: 14	TS: Suresh

Traffic 2011; 0: 0–0

© 2011 John Wiley & Sons A/S

doi:10.1111/j.1600-0854.2011.01165.x

Rab GTPases Regulating Phagosome Maturation Are Differentially Recruited to Mycobacterial Phagosomes

Shintaro Seto[1], Kunio Tsujimura[1] and Yukio Koide[1,2,*]

[1]Department of Infectious Diseases, 1-20-1 Handa-yama, Higashi-ku, Hamamatsu 431-3192, Japan
[2]Hamamatsu University School of Medicine, 1-20-1 Handa-yama, Higashi-ku, Hamamatsu 431-3192, Japan
**Corresponding author: Yukio Koide, koidelb@hama-med.ac.jp*

Mycobacterium tuberculosis (_M. tb_) is an intracellular pathogen that can replicate within infected macrophages. The ability of _M. tb_ to arrest phagosome maturation is believed to facilitate its intracellular multiplication. Rab GTPases regulate membrane trafficking, but details of how Rab GTPases regulate phagosome maturation and how _M. tb_ modulates their localization during inhibiting phagolysosome biogenesis remain elusive. We compared the localization of 42 distinct Rab GTPases to phagosomes containing either _Staphylococcus aureus_ or _M. tb_. The phagosomes containing _S. aureus_ were associated with 22 Rab GTPases, but only 5 of these showed similar localization kinetics as the phagosomes containing _M. tb_. The Rab GTPases responsible for phagosome maturation, phagosomal acidification and recruitment of cathepsin D were examined in macrophages expressing the dominant-negative form of each Rab GTPase. LysoTracker staining and immunofluorescence microscopy revealed that Rab7, Rab20 and Rab39 regulated phagosomal acidification and Rab7, Rab20, Rab22b, Rab32, Rab34, Rab38 and Rab43 controlled the recruitment of cathepsin D to the phagosome. These results suggest that phagosome maturation is achieved by a series of interactions between Rab GTPases and phagosomes and that differential recruitment of these Rab GTPases, except for Rab22b and Rab43, to _M. tb_-containing phagosomes is involved in arresting phagosome maturation and inhibiting phagolysosome biogenesis.

Key words: acidification, cathepsin D, macrophage, membrane trafficking, _Mycobacterium tuberculosis_, phagolysosome biogenesis, phagosome maturation, Rab GTPase

Received 25 May 2010, revised and accepted for publication 19 January 2011

Phagocytosis of pathogens by macrophages is an important process of the innate immune response. Pathogens are enveloped by phagocytic membranes to form phagosomes immediately following internalization. The phagosomes are then processed by a series of interactions with endosomes, resulting in phagosome maturation. During phagosome maturation, phagosomes fuse with lysosomes, in a process known as phagolysosome biogenesis, and acquire degradative and microbicidal properties. Several proteins, including the Rab GTPases, play pivotal roles in phagosome maturation and phagolysosome biogenesis (1). Rab5 is associated with phagosomes immediately after phagocytosis and facilitates the recruitment of Rab5 effector proteins, EEA1 and class III phosphatidylinositol-3-phosphate kinase (2). Membrane bound Rab5 is rapidly dissociated from the phagosome after its activation (3). Rab7 appears on the phagosome membrane after Rab5 dissociation and resides on the membrane during phagosome maturation (4). After acquisition of Rab7, phagolysosome biogenesis is accelerated by the recruitment of Rab7-interacting-lysosomal-protein (RILP) to the phagosome (5).

Mycobacterium tuberculosis (*M. tb*) is the causative agent of tuberculosis and has the ability to survive and proliferate in macrophages. Blockage of phagolysosome biogenesis may assist *M. tb* multiplication within infected macrophages (6,7). *Mycobacterium tuberculosis* inhibits the acidification of phagosomes and recruitment of lysosomal hydratases to phagosomes, resulting in avoidance of the degradative and microbicidal properties of phagosomes (8). It has been thought that *M. tb* arrests phagosome maturation at the stage of Rab5–Rab7 conversion (9) on the mycobacterial phagosomes (10,11), because Rab7 was reported to be absent on mycobacterial phagosomes in macrophages (12–15). Sun et al. (16), however, demonstrated Rab7 localization on mycobacterial phagosomes. We have demonstrated that Rab7 is transiently recruited to and subsequently released from *M. tb*-containing phagosomes and that the release of Rab7 limits the recruitment of cathepsin D and RILP (17,18). Other Rab GTPases, Rab14 and Rab22a, were also demonstrated to be involved in the maturation arrest of *M. tb*-containing phagosomes (12,19), suggesting that *M. tb* disturbs the activity of some Rab GTPases regulating phagosome maturation and survives within macrophages.

Rab GTPases are encoded by a family of more than 60 genes and regulate membrane trafficking (20,21). The role of Rab GTPases in the trafficking of endocytosis and exocytosis has been well studied and their function in phagocytosis is being elucidated. Proteomic analysis revealed that several Rab GTPases are recruited to the latex bead-containing phagosomes (22–24). Smith et al. (25) investigated the interaction of a large number of Rab GTPases with phagosomes containing *Salmonella* in HeLa cells. However, there is currently insufficient information about the role of Rab GTPases in professional phagocytotic cells to understand how *M. tb* subverts membrane trafficking

to survive within infected macrophages. In this study, we investigated the localization and function of 42 Rab GTPases in macrophages infected with *S. aureus* and *M. tb* during the progression of phagosome maturation. Through this comprehensive study, we demonstrate that the progression of phagosome maturation is achieved by the association of several Rab GTPases with the phagosome, leading to phagolysosome biogenesis, and that the release and/or dissociation of these Rab GTPases from *M. tb*-containing phagosomes has the relevance to *M. tb*-induced inhibition of phagolysosome biogenesis.

Results

Maturation of S. aureus- *and* M. tb-*containing phagosomes*

We have previously demonstrated that Rab7 controls the recruitment of the major lysosomal hydratase, cathepsin D, to the latex bead-containing phagosomes and that Rab7 is transiently recruited to and subsequently released from *M. tb*-containing phagosomes, suggesting that *M. tb* alters the localization of Rab7 to arrest phagosome maturation (17). In this study, we examined the localization of other Rab GTPases on *M. tb*-containing phagosomes in order to identify those with pivotal roles in phagosome maturation that are affected by the virulent *M. tb*. Raw264.7 macrophages were infected with *S. aureus* or *M. tb* and phagosomal maturation was compared. We confirmed acidification of the phagosomes and the recruitment of cathepsin D to the phagosomes in macrophages infected with *S. aureus* (Figure 1A,B). Both events, however, were inhibited in the macrophages infected with the virulent strain of *M. tb*, strain H37Rv (Figure 1C,D). We also found that the viability of *S. aureus* phagocytosed by macrophages quickly decreased, while *M. tb* was more robust, demonstrating survival and proliferation (Figure 1E). These results indicate that the maturation of the phagosomes containing *M. tb* was inhibited and that *M. tb* proliferated within Raw264.7 macrophages.

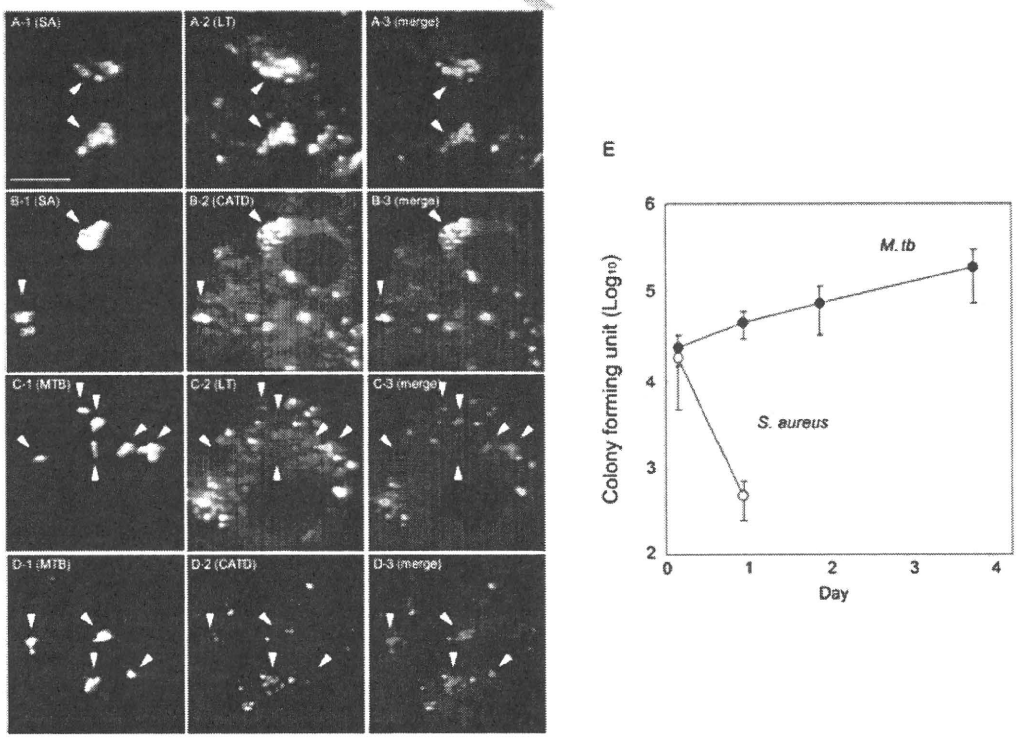

Color

Figure 1: Maturation of phagosomes containing *S. aureus* and *M. tb*. A-D) Acidification and cathepsin D recruitment to phagosomes containing *S. aureus* and *M. tb* were examined. Raw264.7 macrophages were infected with Alexa405-labeled *S. aureus* (A and B) or *M. tb* (C and D) for 6 h. Infected cells were stained with LysoTracker (A and C) or anti-cathepsin D and Alexa488-labeled secondary antibodies (B and D), followed by observation with LSCM. A-1, B-1, C-1 and D-1 show *S. aureus* (SA) or *M. tb* (MTB). A-2, B-2, C-2 and D-2 show localization of LysoTracker (LT) or cathepsin D (CATD). A-3, B-3, C-3 and D-3 show merged images of macrophages and bacteria (merge). Arrows indicate the phagosomes containing SA or MTB. Scale bar, 10 μm. E) Intracellular growth of *S. aureus* and *M. tb* in macrophages. Raw264.7 macrophages (1×10^5 cells) were infected with *M. tb* for 4 h or *S. aureus* for 1 h at an MOI of 10. Infected cells were washed with DMEM three times to remove non-phagocytosed bacteria and then incubated with DMEM containing 10% FBS and 10 μg/mL gentamicin. Infected cells were collected at the indicated days and the number of viable bacteria was determined by a colony forming unit (CFU) counting assay. Data represent the means and standard deviations of three independent experiments. The CFU of *S. aureus* after day 2 was not plotted as they were less than 10.

Localization of Rab GTPases on S. aureus*-containing phagosomes*

To investigate the association of Rab GTPases with *S. aureus* phagosomes, Raw264.7 macrophages were transfected with the expression plasmid for enhanced green fluorescent protein (EGFP)-fused Rab GTPases and were then infected with *S. aureus* labeled with Texas Red. Infected cells were fixed and observed by laser scanning confocal microscopy (LSCM) at the indicated times up to 6 h. More than 100 internalized bacteria within macrophages expressing EGFP-fused Rab GTPase were examined at each time-point. The bacteria surrounded by EGFP signals were regarded as positive phagosomes associated with Rab GTPases. We investigated the kinetics of 42 distinct Rab GTPases whose expression was confirmed in Raw264.7 by reverse transcription-polymerase chain reaction (RT-PCR; data not shown). Their localization is summarized in Table S1 (Supporting information). We found 22 Rab GTPases associated with the phagosomes containing *S. aureus* (Figures 2 and S1). Localization of Rab GTPase could be classified into two types according to their kinetics on *S. aureus*-containing phagosomes, i.e. (i) transient localization or (ii) accumulation.

Figure 2A shows the localization kinetics of Rab GTPases exhibiting type I profiles. Rab5 and Rab22b were recruited to 30 and 90% of the phagosomes at 10 min post-infection (p.i.), respectively. Subsequently, these two Rab GTPases quickly disappeared from the phagosomes. Rab8, Rab8b, Rab11, Rab11b, Rab13, Rab14, Rab20, Rab22a, Rab32, Rab38 and Rab43 also showed transient phagosomal localization, peaking at 30 min and/or 1 h p.i. Figure 2B shows the localization kinetics of Rab GTPases exhibiting type II profiles. Rab7 localized on 40% of the phagosomes at 10 min p.i. The proportion of Rab7-positive phagosomes reached more than 80% at 30 min p.i. and remained at this level at 6 h p.i. as described previously (5,17). Localization of Rab7b, Rab9, Rab9b, Rab34 and Rab39 demonstrated similar kinetics to Rab7 localization. Rab27 and Rab37 did not localize to the phagosomes at the early stage of phagosome maturation. The proportions of Rab27- and Rab37-positive phagosomes increased only after 1 h p.i., suggesting that these Rab GTPases localize on the phagosome at the late stage of phagosome maturation. Rab23 localized on more than 80% of the phagosomes at all time-points investigated. The other 20 Rab GTPases investigated showed no significant associations with the phagosomes (less than 20% of the phagosomes) at all time-points up to 6 h (Figure S2). These results suggest that the network of Rab GTPases regulates the process of phagosome maturation at various time-points.

Localization of Rab GTPases on M. tb*-containing phagosomes*

We next investigated the localization of Rab GTPases on the phagosomes in macrophages infected with the virulent strain of *M. tb*. To investigate the association of Rab GTPases with *M. tb*-containing phagosomes, we infected Raw264.7 macrophages expressing EGFP-fused Rab GTPases with *M. tb* strain H37Rv expressing DsRed (Figure 2 and S1). The localization of Rab GTPases on *M. tb*-containing phagosomes was then examined as described above. Surprisingly, only five of the 22 Rab GTPases (Rab8, Rab8b, Rab9, Rab22b and Rab43) that localized on *S. aureus*-containing phagosomes showed the same localization kinetics on *M. tb*-containing phagosomes. According to the kinetics of localization on *M. tb*-containing phagosomes, the other 17 Rab GTPases were classified into three groups, showing: (i) transient association in contrast to the accumulation on *S. aureus*-containing phagosomes (Rab7, Rab9b, Rab23 and Rab34), (ii) similar kinetics but a lower rate of association than with *S. aureus*-containing phagosomes (Rab7b, Rab14, Rab22a, Rab32, Rab38 and Rab39) and (iii) a very low rate of association (Rab5, Rab11, Rab11b, Rab13, Rab20, Rab27 and Rab37).

Rab7 localized on 40% of *M. tb*-containing phagosomes at 10 min p.i., and the proportion of Rab7-positive *M. tb*-containing phagosomes increased to 80% at 30 min p.i., in a similar way to *S. aureus*-containing phagosomes. The proportion of Rab7-positive *M. tb*-containing phagosomes decreased after 1 h p.i. and reached 30% at 6 h p.i., while the proportion of Rab7-positive *S. aureus*-containing phagosomes remained at 80% up to 6 h p.i., confirming the previous results (17). Similar localization kinetics on *M. tb*-containing phagosomes were observed for Rab9b, Rab23 and Rab34 (type I). Rab7b localized to 40% of *M. tb*-containing phagosomes, as was seen with *S. aureus*-containing phagosomes. Rab7b-positive phagosomes containing *S. aureus* increased to more than 80% up to 6 h p.i., but the proportion of Rab7b-positive phagosomes containing *M. tb* did not change. Rab14, Rab22a, Rab32, Rab38 and Rab39 also showed a weaker association with *M. tb*-containing phagosomes compared with *S. aureus*-containing phagosomes (type II). Rab5 localized on 30% of *S. aureus*-containing phagosomes at 10 min p.i., but the proportion of Rab5-positive *M. tb*-containing phagosomes was less than 20%. Rab11 localized on 80% of *S. aureus*-containing phagosomes at 30 min p.i., but showed no significant association on *M. tb*-containing phagosomes (less than 20%). Rab11b, Rab13, Rab20, Rab27 and Rab37 also showed no significant association with *M. tb*-containing phagosomes (type III). These results suggest that the dissociation of 17 Rab GTPases might disrupt membrane trafficking in the maturation process of *M. tb*-containing phagosomes. We found that 20 Rab GTPases, which were not associated with *S. aureus*-containing phagosomes, also showed no significant association with *M. tb*-containing phagosomes (Figure S2).

Localization of Rab GTPases on isolated phagosomal fractions

To examine the recruitment of endogenous Rab GTPases to the phagosomes, we conducted immunoblotting analysis to detect Rab GTPases in isolated phagosomes containing latex beads and *M. tb*. Raw264.7 macrophages were allowed to phagocytose latex beads or infected with

Uncorrected Proof

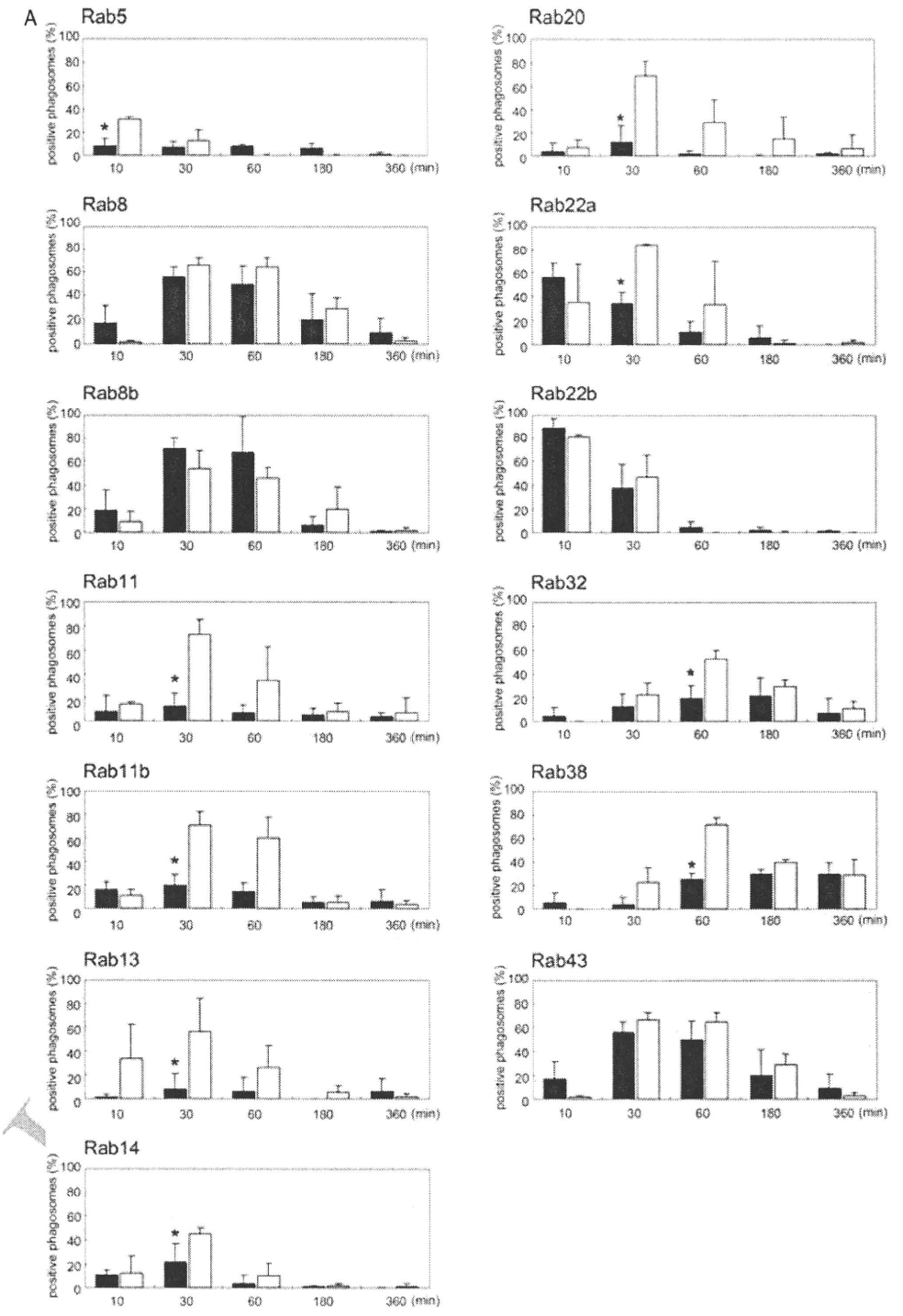

Figure 2: Localization kinetics of Rab GTPases on *M. tb*- and *S. aureus*-containing phagosomes. The proportions of Rab GTPase-positive phagosomes containing *M. tb* and *S. aureus* were examined at the indicated time-points p.i. Data represent the means and standard deviations of three independent experiments in which more than 100 phagosomes were counted for each condition. Rab GTPases were classified into two types according to their localization on *S. aureus*-containing phagosomes as follows: (A) Rab GTPases transiently localizing to the phagosomes and (B) Rab GTPases consecutively or accumulatively localizing to the phagosomes. Black and white bars indicate the proportion of Rab-positive phagosomes containing *M. tb* and *S. aureus*, respectively. *$p < 0.05$ (unpaired Student's *t*-test).

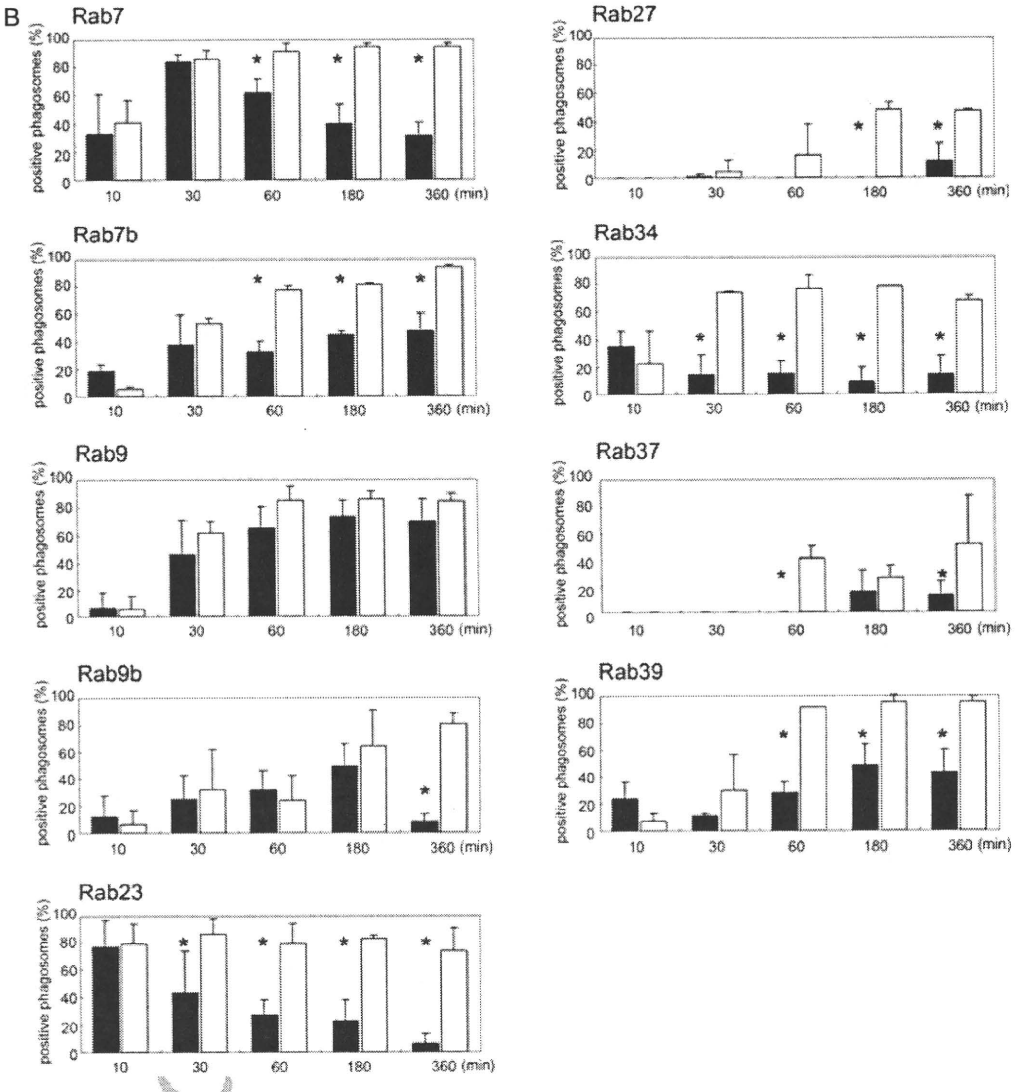

Figure 2: *Continued.*

M. tb for 2 or 8 h. Phagosomal fractions were isolated as previously reported (26,27). We confirmed that the phagosomal fractions were not contaminated with other subcellular organelles using electron microscopy (Figure 3A) as shown previously (17). Immunoblotting analysis revealed that Rab5, Rab7, Rab9, Rab14 and Rab22a were recruited to both phagosomal fractions (Figure 3B). We quantified the band intensities corresponding to Rab GTPases in latex bead- and *M. tb*-containing phagosomal fractions at 2 and 8 h p.i. to follow the dynamics of Rab GTPases on the phagosomes (Figure 3C). In the latex bead-containing phagosomes, the amounts of Rab5, Rab7, Rab9 and Rab22a at 8 h showed no change or slightly decreased in comparison with those at 2 h, whereas the amount of Rab14 at 8 h decreased significantly to about 30% of that at 2 h. In *M. tb* phagosomal fractions, the amounts of Rab5, Rab7, Rab14 and Rab22a at 8 h demonstrated significant decreases to about 40, 20, 60 and 30% of those at 2 h, respectively. Rab9 did not show significant changes in *M. tb* phagosomal fractions. These results suggest that Rab5, Rab7, Rab9 and Rab22a are associated with the latex bead-containing phagosomes, but these Rab GTPases except for Rab9 are subsequently released from *M. tb*-containing phagosomes, and that recruited Rab14 is dissociated from both phagosomes.

A network of Rab GTPases regulating phagosome maturation

To examine the contribution of 22 Rab GTPases localizing to *S. aureus*-containing phagosomes during phagosome maturation, Raw264.7 macrophages were transfected with two expression plasmids for EGFP and the

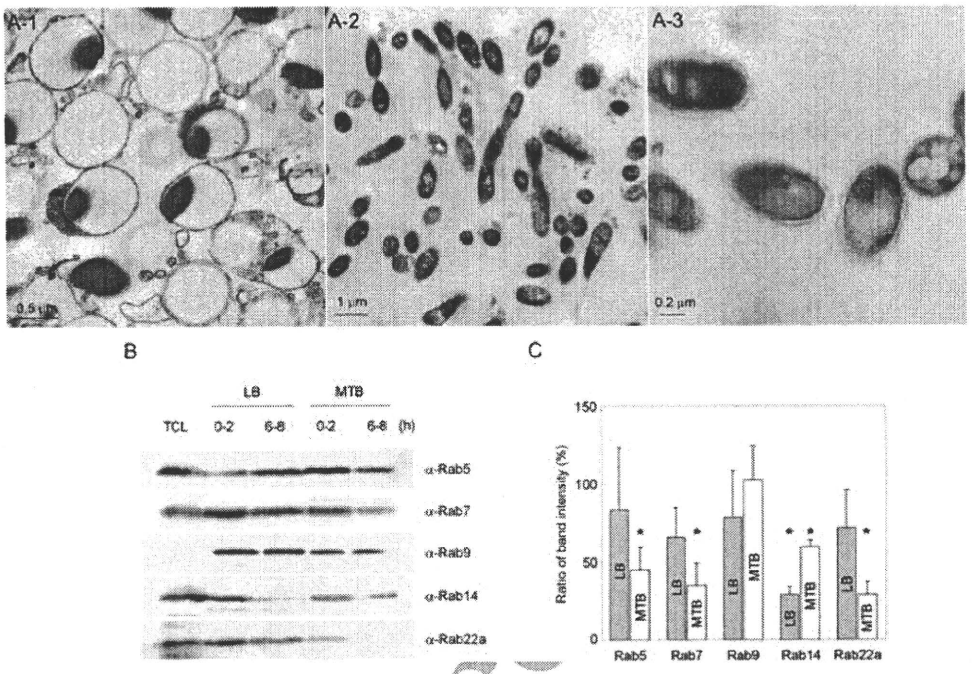

Figure 3: Rab GTPases localization in isolated *M. tb* phagosomal fractions. A) Thin-section electron micrographs of isolated phagosomal fractions containing the latex beads (A-1) and *M. tb* (A-2, A-3) for 6 h. B) Immunoblotting analysis of latex bead and *M. tb* phagosomal fractions with antibodies to Rab5, Rab7, Rab9, Rab14 and Rab22a is shown. Latex beads (LB) or *M. tb* (MTB) were internalized for 2 h and phagosomal fractions were collected immediately (0–2 h) or after further incubation for 6 h (6–8 h). Total cell lysates from Raw264.7 (TCL) and phagosomal fractions were subjected to SDS–PAGE, followed by immunoblotting analysis using the indicated antibodies. C) Ratios of band intensity for Rab GTPase at 6–8 h relative to that at 0–2 h in phagosomal fractions. Gray and white bars show the ratio of band intensity of indicated Rab at 6–8 h as compared to that at 0–2 h in latex bead and *M. tb* phagosomal fractions, respectively. Data represent the means and standard deviations of three independent experiments. *$p < 0.05$ (paired Student's *t*-test).

dominant-negative (DN) form of each Rab gene. For the evaluation of phagosome maturation, we determined the degree of phagosomal acidification and the recruitment of cathepsin D to the phagosome, because both events were exceedingly inhibited in the phagosomes containing *M. tb* H37Rv in macrophages (Figure 1). Transfected cells were allowed to phagocytose latex beads for 3 h, then acidification of the phagosome was investigated (Figure 4). Phagocytosing cells were stained with LysoTracker and its accumulation within phagosomes was observed by LSCM. Phagosomal acidification was clearly observed in control cells (Figure 4A). We found that phagosomal acidification was inhibited by Rab7DN as described previously (5), confirming that the experiment was being conducted correctly. Expression of Rab20DN or Rab39DN also inhibited the accumulation of LysoTracker within the phagosomes (Figure 4B,C). We quantified the fluorescent density of LysoTracker accumulated in phagosomes relative to that in other endosomal/lysosomal (E/L) components of transfected cells expressing DN forms of Rab GTPases (Figure 4D). As expected, the expression of Rab7DN, Rab20DN and Rab39DN decreased the fluorescent ratio in comparison with that in the control cells. These results suggest that Rab7, Rab20 and Rab39 function in phagosomal acidification. The mean fluorescence intensities derived from LysoTracker staining were not affected by the expression of Rab7DN, Rab20DN or Rab39DN (Figure S3), indicating that expression of these DN forms of Rab GTPases had no effect on the generation of acidic vacuoles in macrophages.

We next examined the recruitment of cathepsin D to the phagosomes in macrophages expressing DN forms of the Rab GTPases (Figure 5). Transfected cells were allowed to phagocytose latex beads for 3 h and were then stained with an anti-cathepsin D antibody. Stained cells were observed by LSCM. Cathepsin D was recruited to the phagosome in the control cells (Figure 5A). The recruitment of cathepsin D was inhibited by the expression of Rab7DN as described previously (17). Immunofluorescence microscopy also demonstrated that the expression of Rab20DN, Rab22bDN, Rab32DN, Rab34DN, Rab38DN or Rab43DN inhibited the recruitment of cathepsin D to the phagosomes (Figure 5B,C). The ratiometric quantification revealed that the expression of these DN forms of Rab GTPases decreased the association of cathepsin D with phagosomes (Figure 5D). Immunoblotting analysis revealed that the amount of products and the processing

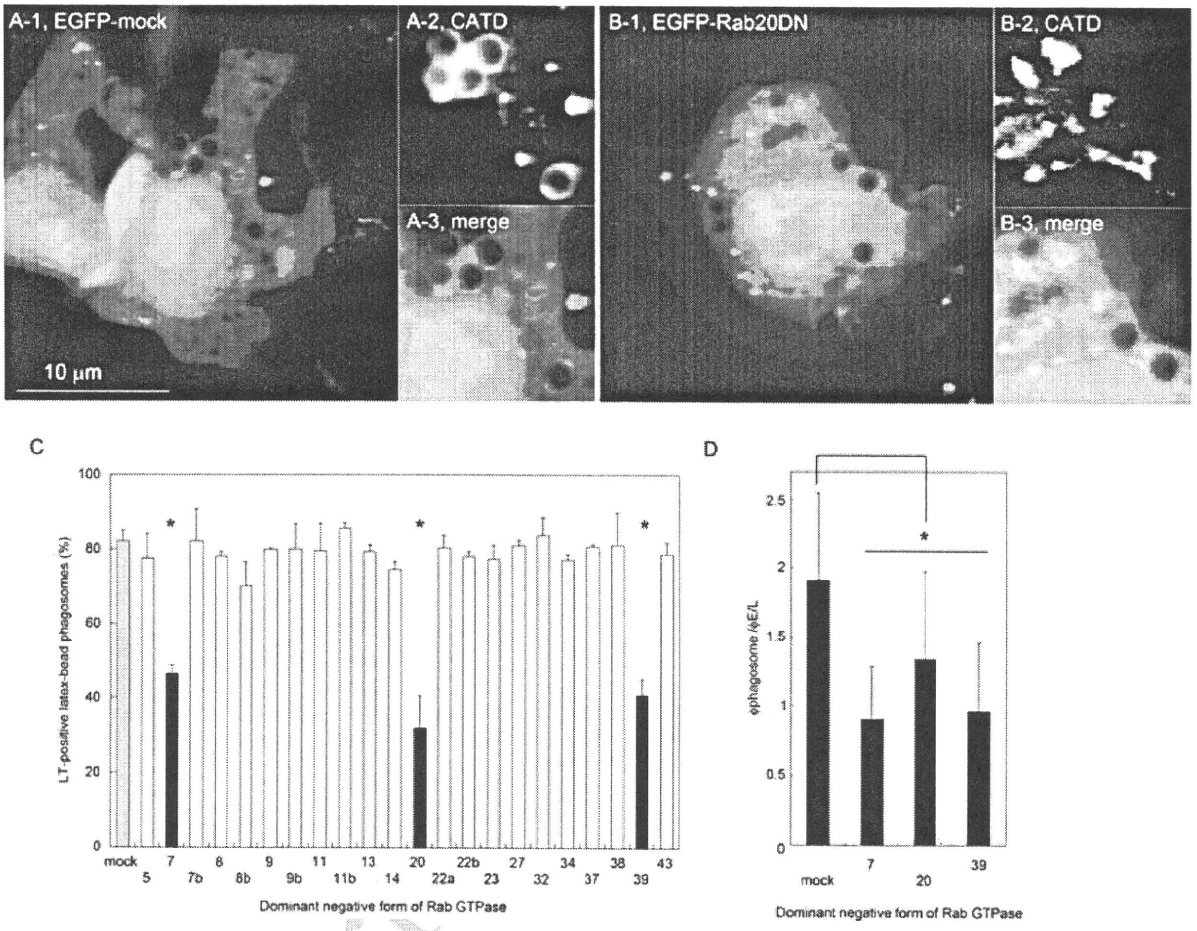

Figure 4: Phagosomal acidification in macrophages expressing the DN forms of Rab GTPases. Raw264.7 macrophages were transfected with plasmids encoding EGFP and control vector (mock) (A) or the DN form of Rab20 (Rab20DN) (B). Transfected cells were allowed to phagocytose latex beads for 3 h and were then stained with LysoTracker (LT). Stained cells were observed by LSCM. Enlarged images of the latex bead-containing phagosomes in A-1 and B-1 are represented in A-2, A-3 and B-2, B-3, respectively. C) The proportion of LysoTracker-positive phagosomes in macrophages expressing the DN forms of Rab GTPases. Data represent the means and standard deviations of three independent experiments in which more than 100 phagosomes were counted for each condition. D) Ratiometric quantification of fluorescent density of LysoTracker associated with the phagosomes (φphagosome) relative to that of other φE/L components. Data represent the means and standard deviations of three independent experiments in which more than 100 phagosomes were examined for each condition. *$p < 0.05$ (unpaired Student's *t*-test).

of cathepsin D did not change significantly in the cells expressing the DN forms of the Rab GTPases as compared with the control cells (data not shown). These results suggest that Rab7, Rab20, Rab22b, Rab32, Rab34, Rab38 and Rab43 regulate the recruitment of cathepsin D to the phagosomes.

Constitutively active forms of Rab GTPases were dissociated from M. tb*-containing phagosomes*

To elucidate the mechanism by which Rab GTPases are dissociated from *M. tb*-containing phagosomes, we examined the localization of the constitutively active (CA) forms of Rab GTPases regulating phagosome maturation on *M. tb*-containing phagosomes. We previously demonstrated that Rab7CA is released from *M. tb*-containing phagosomes (17). In this study, we found that the recruitment of Rab20CA, Rab32CA, Rab34CA, Rab38CA and Rab39CA to *M. tb*-containing phagosomes is also impaired, in a similar way to the wild-type versions of these Rab GTPases (data not shown). We next examined the fusion of *M. tb*-containing phagosomes with lysosomes in macrophages expressing the CA forms of the Rab GTPases (Figure 6). Macrophages transfected with the expression plasmids for EGFP and each CA of Rab GTPase were preloaded with Texas Red-dextran and then infected with Alexa405-fluorophore-labeled *M. tb* for 6 h. Lysosomes did not fuse with the phagosomes containing live *M. tb* in macrophages expressing Rab7CA, Rab20CA, Rab32CA, Rab34CA, Rab38CA or Rab39CA

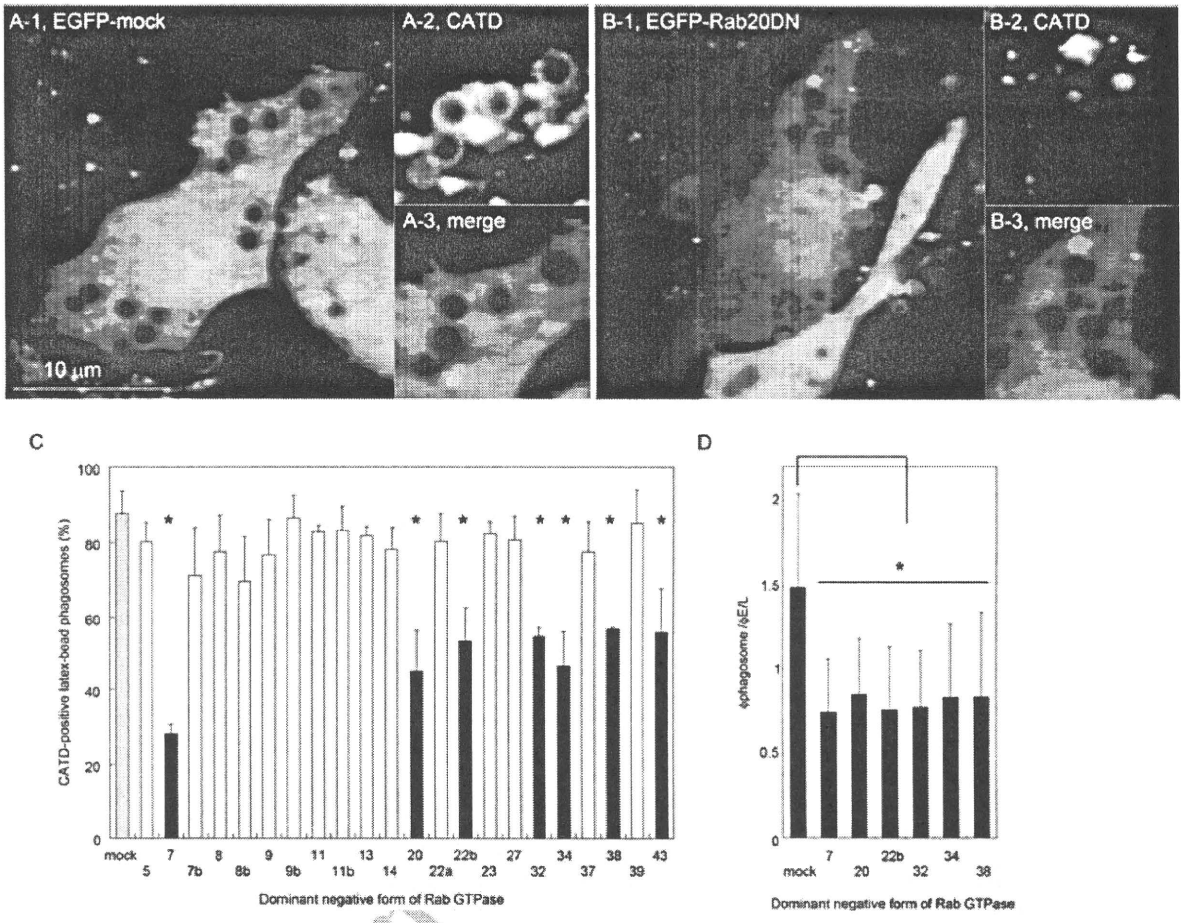

Color

Figure 5: Cathepsin D recruitment to phagosomes in macrophages expressing the DN form of Rab GTPases. Raw264.7 macrophages were transfected with plasmids encoding EGFP and control vector (mock) (A) or Rab20DN (B). Transfected cells were allowed to phagocytose latex beads for 3 h and were then stained with anti-cathepsin D (CATD) and Alexa568-conjugated secondary antibodies. Stained cells were observed by LSCM. Enlarged images of the latex bead-containing phagosomes in A-1 and B-1 are represented in A-2, A-3 and B-2, B-3, respectively. C) The proportion of cathepsin D-positive phagosomes in macrophages expressing the DN forms of Rab GTPases. Data represent the means of three independent experiments in which more than 100 phagosomes were counted for each condition. D) Ratiometric quantification of fluorescent density of cathepsin D associated with the phagosomes (φphagosome) relative to that of other φE/L components. Data represent the means and standard deviations of three independent experiments in which more than 100 phagosomes were examined for each condition. *$p < 0.05$ (unpaired Student's *t*-test).

(Figure 6 and data not shown). Taken together, these results suggest that these Rab GTPases are not directly targeted by *M. tb* for inhibition of phagolysosome biogenesis and suggest instead that the difference in the localization of Rab GTPases between *S. aureus*- and *M. tb*-containing phagosomes is due to difference in how the phagosomes change or evolve over time.

Localization of Rab GTPases on phagosomes containing an avirulent M. tb *strain*

To investigate the correlation between the dissociation of Rab GTPases and the arrest of phagosome maturation, we examined the localization of Rab GTPases on phagosomes containing an attenuated strain, *M. tb* H37Ra. The proliferative activity of *M. tb* H37Ra, within infected macrophages was reduced compared with that of the virulent *M. tb* H37Rv strain (data not shown), suggesting that the inhibition of phagolysosome biogenesis was suppressed in macrophages infected with *M. tb* H37Ra. We examined the fusion of *M. tb* H37Ra phagosomes with lysosomes in infected macrophages. Raw264.7 macrophages were preloaded with Texas Red-dextran, infected with *M. tb* strain H37Ra for 6 h and then observed by LSCM. Stronger fluorescent signals derived from dextran were observed within the phagosomes containing *S. aureus*. The fluorescent signals on *M. tb* H37Ra phagosomes were weaker than those on *S. aureus*-containing phagosomes but stronger than those on *M. tb* H37Rv phagosomes (Figure 7A–D). These results suggest that *M. tb* H37Ra phagosomes have the intermediate

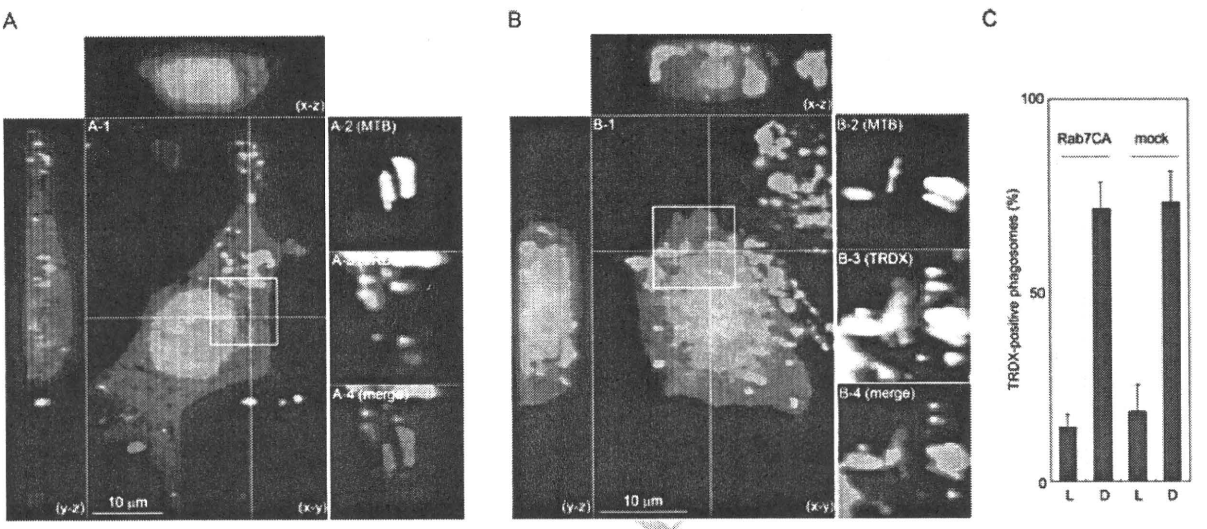

Color

Figure 6: Impairment of fusion of lysosomes with *M. tb*-containing phagosomes in macrophages expressing the CA form of Rab7. Raw264.7 macrophages were transfected with plasmids expressing EGFP and the CA form of Rab7 (Rab7CA). Transfected cells were preloaded with Texas Red-dextran (TRDX) to label lysosomal vesicles, followed by incubation with live (A) and dead (B) *M. tb* labeled with Alexa405-fluorophore for 6 h. Fixed cells were observed by LSCM. Projections of focal planes with *y–z* and *x–z* side views show the sequestration and colocalization of fluorescent dextrans with *M. tb*-containing phagosomes in (A) and (B), respectively. Enlarged images showing the *M. tb*-containing phagosomes of A-1 are presented in A-2, A-3 and A-4. Enlarged images showing the *M. tb*-containing phagosomes of B-1 are shown in B-2, B-3 and B-4. A-2 and B-2 show live and dead *M. tb* (MTB), respectively. B-3 and C-3 show the localization of fluorescent dextran (TRDX). A-4 and B-4 show the merged images of macrophages and bacteria (merge). Scale bar, 10 μm. C) The proportion of *M. tb*-containing phagosomes labeled with Texas Red-dextran in macrophages expressing Rab7CA. Macrophages transfected with the plasmid expressing Rab7CA or control vector (mock) were incubated with live (L) or dead (D) *M. tb* for 6 h. Data represent the means of three independent experiments in which more than 100 phagosomes were counted for each condition.

AQ3

ability to fuse with lysosomal vesicles compared with *M. tb* H37Rv and *S. aureus*-containing phagosomes. We finally examined the association of Rab GTPases regulating phagosome maturation with phagosomes containing *M. tb* strain H37Ra. Macrophages expressing EGFP-Rab GTPases found to be involved in phagosome maturation were infected with Texas Red-labeled *M. tb* strain H37Ra or H37Rv for 6 h. The proportions of Rab7-, Rab20-, Rab34- and Rab39-positive phagosomes containing *M. tb* strain H37Ra were significantly higher than those of phagosomes containing *M. tb* strain H37Rv (Figure 7E), although those were lower than those of phagosomes containing *S. aureus* (Figure 2). These results suggest that *M. tb* strain H37Ra impairs the association of Rab GTPases regulating phagosome maturation to phagosomes, but less severely than *M. tb* strain H37Rv, leading to reduced fusion of lysosomal vesicles with phagosomes.

Discussion

Intracellular pathogens are known to disrupt the normal membrane trafficking pathway of the host cell, with this alteration possibly contributing toward more hospitable intracellular conditions for their growth and multiplication. Rab GTPases play pivotal roles in membrane trafficking (20,21). Therefore, the activity and localization of these regulatory proteins may be targeted by intracellular pathogens to establish a niche for their proliferation (28). Several reports have investigated the localization of Rab5 and Rab7 on mycobacterial phagosomes (14–17,29,30), because Rab5 and Rab7 localize to the phagosome and co-ordinately contribute to the control of phagosome maturation (1). The localization of Rab14 and Rab22a on mycobacterial phagosomes was also shown to regulate early stages of phagosome maturation (12,19). However, little is known about how mycobacteria subvert the network of Rab GTPases regulating phagosome maturation within infected macrophages. In this study, we compared the subcellular localization of 42 distinct Rab GTPases on *M. tb*-containing phagosomes with that on *S. aureus*-containing phagosomes in macrophages to further understand how mycobacteria disrupt membrane trafficking in phagosomes.

We found that 22 Rab GTPases were recruited to *S. aureus*-containing phagosomes and that 17 of these Rab GTPases showed different localization kinetics on *M. tb*-containing phagosomes (Figure 2). We also found that some Rab GTPases localizing to phagosomes regulated phagosomal acidification and the recruitment of cathepsin D to the phagosome (Figures 4 and 5). This is the first report demonstrating that Rab20, Rab22b, Rab32, Rab34, Rab38, Rab39 and Rab43 regulate phagosome

Uncorrected

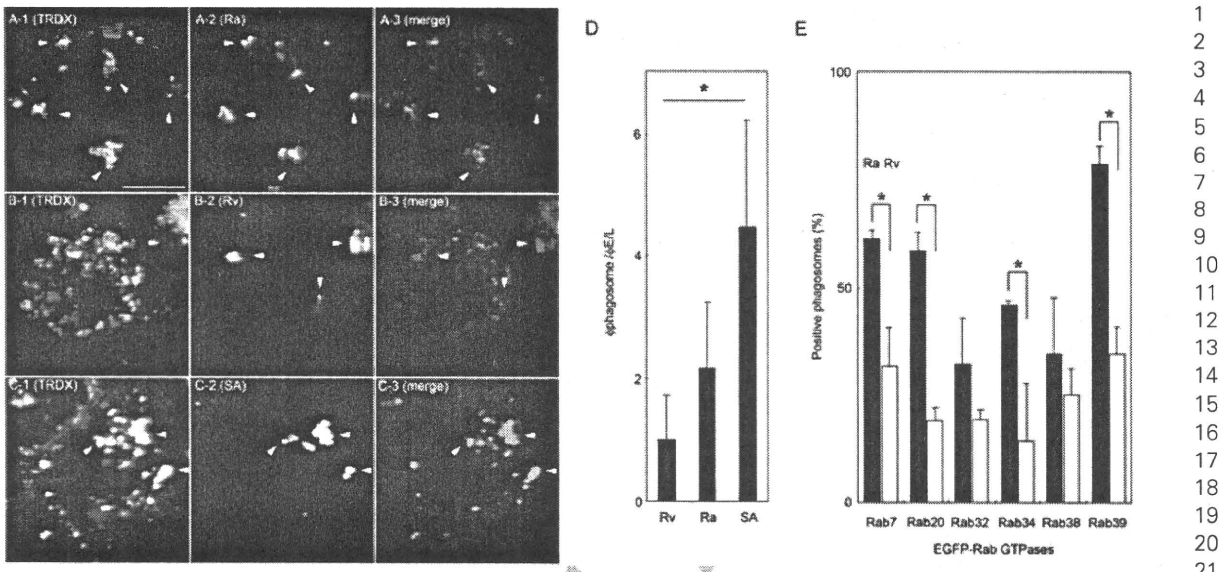

Color

Figure 7: Accession of lysosomes with the phagosomes correlates with phagosomal localization of Rab GTPases regulating phagosomal maturation. A–C) Raw264.7 macrophages preloaded with Texas Red-dextran were infected with (A) *M. tb* strain H37Ra (Ra), (B) *M. tb* strain H37Rv (Rv) and (C) *S. aureus* (SA) labeled with Alexa405-fluorophore for 6 h. Fixed cells were observed by LSCM. A-1, B-1 and C-1 show macrophages labeled with fluorescent dextran. A-2, B-2 and C-2 show bacteria labeled with Alexa405-fluorophore. A-3, B-3 and C-3 show the merged images of macrophages and bacteria. Arrows and arrowheads demonstrate phagosomes with and without fluorescent dextran-labeled lysosomal vesicles, respectively. Scale bar, 10 μm. D) Ratiometric quantification of fluorescent dextran within the phagosomes relative to that of other E/L components. The ratio of fluorescent density within the phagosomes (φphagosome) relative to that of other E/L components (φE/L) was shown. Data represent the means and standard deviations of three independent experiments in which more than 100 phagosomes were examined for each condition. *$p < 0.05$ (Tukey–Kramer multiple comparison test). E) Recruitment of Rab GTPases regulating phagosome maturation of *M. tb* strains H37Ra (Ra) and H37Rv (Rv). Raw264.7 macrophages were transfected with plasmids encoding EGFP-fused Rab GTPases. Macrophages were infected with *M. tb* strains H37Ra or H37Rv labeled with Texas Red, fixed at 6 h (Rab7, Rab34 and Rab39), 1 h (Rab32 and Rab38) and 30 min (Rab20), and then observed by LSCM. Data represent the means and standard deviations of three independent experiments in which more than 100 phagosomes were counted for each condition. *$p < 0.05$ (unpaired Student's *t*-test).

maturation. Rab22b, Rab32, Rab34 and Rab38 were reported to localize to the trans-Golgi network (31–33). We found that these Rab GTPases showed various association and dissociation kinetics with the phagosomes (Figure 2A) and were involved in the recruitment of cathepsin D to the phagosome. Our observations are consistent with a previous report showing the direct transport of cathepsin D from the trans-Golgi network to the phagosome (34). Rab34 is also reported to interact with RILP (32), suggesting its involvement in the promotion of phagolysosome biogenesis. In the present study, Rab43, a regulator of endoplasmic reticulum–Golgi trafficking (35), was also found to regulate the recruitment of cathepsin D to the phagosome. Rab20 was reported to localize to the endoplasmic reticulum (36) and colocalize with vacuolar-type ATPases (37). Additionally, we demonstrated the involvement of Rab20 in both phagosomal acidification and cathepsin D recruitment. We also found that Rab39 regulates phagosomal acidification and colocalizes with lysosomes (Table S1). Considering its recruitment kinetics to the phagosomes (Figure 2), Rab39 seems to maintain the phagosomal acidification at the late stage of phagocytosis. These observations, taken together, suggest that these Rab GTPases differentially regulate phagosome maturation at the various stages of phagocytosis.

Rab5 is widely accepted as a marker of mycobacterial phagosomes in infected macrophages (14,15). In this study, we found that Rab5 is not recruited to *M. tb*-containing phagosomes at 10 min p.i. (Figure 2). However, Kelley and Schorey (15) investigated Rab5 recruitment to the phagosomes containing *Mycobacterium avium* using a retrovirus transduction system. A previous live cell imaging analysis revealed that Rab5 is transiently associated with and then dissociated from mycobacterial phagosomes immediately after infection (12). We also found that Rab5 was recruited to approximately 40% of phagosomes containing *Mycobacterium bovis* strain bacille Calmette–Guérin (BCG) in Raw264.7 macrophages at 10 min p.i. (Figure S4). These results suggest that the kinetics of Rab5 recruitment to the phagosomes is different between the mycobacteria infected. Inconsistent with the fluorescent microscopic analysis, Rab5 could be detected in phagosomal fractions containing *M. tb* and latex beads by immunoblotting analysis at 6 h p.i. (Figures 2 and 3). Desjardins et al. (27) showed that recruited Rab5 to the

Uncorrected

latex bead-containing phagosome decreases continuously over time. Via et al. (14) also reported that recruited Rab5 to the phagosomes containing latex beads or *M. bovis* BCG decreases over time but detectable by immunoblotting analysis. It is likely that the detection of Rab5 recruitment to the phagosomes at 6 h p.i. in our study is caused by the high sensitivity of immunoblotting analysis.

Rab7 localization on mycobacterial phagosomes has been controversial for a long time. Rab7 was reported to be absent from mycobacterial phagosomes in macrophages (12–15). Clemens et al. (29) reported that Rab7 localizes to *M. tb*-containing phagosomes in HeLa cells, but they also mentioned that Rab7 localization is caused by its overexpression. Sun et al. (16) demonstrated that Rab7 localizes to phagosomes containing *M. bovis* BCG in Raw264.7 macrophages. Recently, proteomic analysis also revealed that Rab7 localizes to the phagosomes containing *M. bovis* BCG in a human monocyte cell line (38). Rab7 depletion by RNA interference increased the proliferation of *Mycobacterium fortuitum* in *Drosophila* S2 cells (39), but did not affect proliferation of *M. tb* in a human monocyte cell line (40). These results suggest that Rab7 localizes to phagosomes containing avirulent mycobacteria, but not to those containing virulent mycobacteria, leading to inhibition of avirulent mycobacterial proliferation. Our previous and current studies demonstrated that Rab7 is transiently recruited to, and subsequently released from *M. tb*-containing phagosomes using imaging and immunoblotting analyses (Figures 2 and 3) (17). This dissociation would invalidate Rab7-mediated inhibition of *M. tb* proliferation in macrophages. We found that Rab20 shows a very weak localization to *M. tb*-containing phagosomes and regulates both phagosomal acidification and recruitment of cathepsin D (Figures 2, 4 and 5). The recruitment of Rab20 to *S. aureus*-containing phagosomes occurs transiently at 30 min after phagocytosis, when Rab7 recruitment coincides. We confirmed that the expression of Rab7DN and Rab20DN did not inhibit the recruitment of Rab20 and Rab7, respectively (data not shown), indicating that they independently contribute to phagosome maturation. Considering that Rab7 depletion inhibits the biogenesis of lysosomes (41), the function of Rab7 in the biogenesis of lysosomes has a significant connection to phagosome maturation and phagolysosome biogenesis. This finding raises the possibility that Rab20 contributes to phagosome maturation in other ways such as the biogenesis of late endosomes or lysosomes. Taken together, these results suggest that the dissociation of Rab7 and Rab20 from *M. tb*-containing phagosomes contributes to arresting the maturation of *M. tb*-containing phagosomes.

Transferrin receptors remain on mycobacterial phagosomes as a result of phagosomal fusion with early endosomal vesicles (42). In this study, we found that Rab11a and Rab11b are transiently recruited to *S. aureus*-containing phagosomes, but not *M. tb*-containing phagosomes (Figure 2). According to the evidence that Rab11 is involved in the recycling of transferrin receptors (43), the failure to recruit Rab11a/b might be one of the reasons why transferrin receptors are associated with *M. tb*-containing phagosomes. Rab14 and Rab22a were reported to localize to mycobacterial phagosomes and arrest phagosome maturation (12,19). In this study, we found that these Rab GTPases were transiently recruited to *M. tb*-containing phagosomes through imaging and immunoblotting analyses (Figures 2 and 3). Our results also showed that Rab14 and Rab22a were recruited to *S. aureus*- and the latex bead-containing phagosomes (Figures 2 and 3), while other imaging analyses showed no localization of these Rab GTPases to latex bead or inactivated mycobacterial phagosomes (12,19). Certain proteomic analysis results support the association of these Rab GTPases with the latex bead-containing phagosomes (22–24). It is possible that the differing results between imaging and immunoblotting analyses of Rab14 and Rab22a recruitment to the latex-bead phagosome were caused by the emphasizing effect of our imaging analysis due to overexpression of GFP fusion proteins. We also found that the CA and DN forms of these Rab GTPases had no influence on the fusion of lysosomal vesicles with phagosomes containing *S. aureus* or *M. tb* (data not shown). These results suggest that Rab14 and Rab22a are passive markers for the progression of phagosome maturation.

Some Rab GTPases that were not recruited to phagosomes containing a virulent *M. tb* strain were actively associated with phagosomes containing the avirulent *M. tb* strain H37Ra (Figure 7E) or *M. bovis* BCG (data not shown). In parallel with the recruitment of Rab GTPases regulating phagosome maturation, the ability of *M. tb* H37Ra to inhibit phagolysosome biogenesis was weaker than that of *M. tb* H37Rv (Figure 7A–D). These findings raise the possibility that the recruitment of Rab GTPases to virulent *M. tb*-containing phagosomes is modulated. It is known that ESAT-6 secretion is inhibited in *M. tb* strain H37Ra (44), and that *M. bovis* BCG lacks the RD-1 region encoding genes for ESAT-6 and secretion machineries for ESAT-6 and other secretory proteins (ESX-1) (45). These observations suggest that virulence proteins secreted by ESX-1 directly or indirectly control the dissociation of Rab GTPases from *M. tb*-containing phagosomes. Of these virulent proteins, ESAT-6 may be involved in the dissociation of Rab GTPases from *M. tb*-containing phagosomes, as it is reported to induce pore formation on biomembranes (46). Pore formation in phagosomal membranes may cause the instability or dissociation of Rab GTPases anchoring to the phagosomes.

Cardoso et al. (47) reported that Rab10 regulates phagosome maturation and does not localize to phagosomes containing *M. bovis* BCG. They also reported that the expression of CA or DN forms of Rab10 modulates the maturation of mycobacterial phagosomes (47). We observed that about 10% of *S. aureus*-containing phagosomes, but less than 1% of *M. tb*-containing phagosomes acquire Rab10 at 10 min p.i. (Figure S4). We did not

Uncorrected Proof

examine the function of Rab10 in phagosome maturation in detail in this study because the association of Rab10 to the phagosome was very weak in our experimental system.

In conclusion, we propose a model in which the network of Rab GTPases regulates phagosome maturation, and the recruitment of Rab GTPases are modulated by phagosomes containing *M. tb* during inhibition of phagolysosome biogenesis (Figure S5). At least 22 Rab GTPases localize on the phagosome transiently or consecutively during progression of phagosome maturation, with Rab7, Rab20 and Rab39 regulating acidification of the phagosome. Rab7, Rab20, Rab22b, Rab32, Rab34, Rab38 and Rab43 regulate the recruitment of cathepsin D to the phagosome. The recruitment of these Rab GTPases to *M. tb*-containing phagosomes is modulated, except for Rab22b and Rab43. The current study does not support that *M. tb* directly targets these Rab GTPases during *M. tb*-induced inhibition of phagolysosome biogenesis, but suggests that the modulation of the recruitment of Rab GTPases to *M. tb*-containing phagosomes is involved in the arrest of phagosome maturation and inhibition of phagolysosome biogenesis. We are currently investigating the roles of these Rab GTPases in phagolysosome biogenesis to further understand how *M. tb* evades killing activities within the phagosome.

Materials and Methods

Cell and bacterial cultures

Raw264.7 macrophages were obtained from the American Type Culture Collection and maintained in DMEM (Sigma-Aldrich) supplemented with 10% FBS (Invitrogen), 25 μg/mL penicillin G and 25 μg/mL streptomycin, at 37°C under 5% CO_2. *M. tb* strains, H37Rv and H37Ra, were obtained from Japan Research Institute of Tuberculosis. *M. bovis* BCG Tokyo was obtained from Japan BCG Laboratory. *M. tb* strains H37Rv and H37Ra, and *M. bovis* BCG, were grown to mid-logarithmic phase in 7H9 medium supplemented with 10% Middlebrook ADC (BD Biosciences), 0.5% glycerol and 0.05% Tween 80 (*Mycobacterium* complete medium) at 37°C. *M. tb* transformed with a plasmid encoding DsRed (48) was grown in *Mycobacterium* complete medium containing 25 μg/mL kanamycin. *S. aureus* was grown in brain heart infusion broth (BD Biosciences) at 37°C.

Bacteria labeling

M. tb and *S. aureus* were labeled with Texas Red or Alexa405 (Invitrogen) as described previously (49), with minor modifications. Briefly, bacterial cultures were centrifuged for 5 min at 8000 × ***g*** and washed with PBS three times. Bacterial cells were then labeled with 20 μg/mL Texas Red ester or 100 μg/mL Alexa405 succinimidyl ester in PBS at 37°C for 30 min, followed by washing with PBS containing 0.05% Tween 80 for mycobacteria and PBS for *S. aureus*. Labeled bacteria were then suspended in DMEM with 10% FBS and incubated at 37°C for 30 min. Bacterial suspensions were passed through a 26-gauge needle 10 times and centrifuged for 5 min at 1000 × ***g*** to remove clumps and aggregates. If necessary, *M. tb* was heat inactivated before labeling with fluorescent dyes by incubation at 90°C for 10 min. The viability of heat-inactivated *M. tb* cells were confirmed as less than 1% of that of nontreated bacteria by a colony counting assay. *Mycobacterium tuberculosis* expressing DsRed was washed three times with PBS containing 0.05% Tween 80, and then a single cell suspension was prepared. The viability of inoculated bacteria labeled with fluorescent dyes or expressing DsRed was confirmed more than 99% by staining with SYTOX Green (Invitrogen).

Infection of bacteria

Transfected cells grown on round coverslips in 12-well plates were infected with bacteria. Bacterial cells were washed with PBS containing 0.05% Tween 80 three times and suspended in DMEM with 10% FBS at a multiplicity of infection (MOI) of 10–30. Aliquots of 1 mL of bacterial suspension were added to 3×10^5 cells of Raw264.7 macrophages on coverslips in 12-well plates, followed by centrifugation at 150 × ***g*** for 5 min and incubation for 10 min at 37°C. Infected cells on coverslips were washed with DMEM three times to remove non-phagocytosed bacteria and then incubated with DMEM containing 10% FBS. At the indicated time-points, infected cells were fixed with 1 or 3% paraformaldehyde in PBS.

Antibodies

Rabbit anti-Rab5 polyclonal antibody (Abcam), mouse anti-Rab7 monoclonal antibody (Abcam), rabbit anti-Rab9 monoclonal antibody (Abcam), rabbit anti-Rab14 polyclonal antibody (Sigma-Aldrich), rabbit anti-Rab22a polyclonal antibody (Proteintech Group, Inc.), rat anti-mouse LAMP-2 monoclonal antibody (SouthernBiotech) and goat anti-mouse cathepsin D polyclonal antibody (R&D systems) were all purchased. Alexa488- and Alexa546-conjugated anti-IgG antibodies (Invitrogen) were purchased. AQ4

Isolation of the latex bead- and M. tb-containing phagosomes

Eight 15-cm plates of Raw264.7 macrophages were used for each condition. For isolation of latex-bead phagosomal fractions, latex beads (0.7 μm, Polysciences, Inc.) were added to cells for 2 h, washed three times with prewarmed DMEM. For preparation of 2- or 8-h phagosomal fractions, cells were collected immediately after washing or further incubated in DMEM with 10% FBS, respectively. Collected cells were lysed and subjected to discontinuous sucrose gradient centrifugation as described previously (27). For isolation of *M. tb* phagosomal fractions, bacteria at an MOI of 30 were infected to Raw264.7 for 2 h, washed and then incubated for the indicated times. Infected cells were collected, lysed and subjected to fractionation as described previously (26). Both phagosomal fractions were extracted by RIPA buffer containing 25 mM Tris–HCl pH 7.6, 150 mM NaCl, 1% Nonidet P-40, 1% sodium deoxycholate and 0.1% SDS. We confirmed that mycobacterial proteins arenot extracted by RIPA buffer as described previously (38). AQ5 For immunoblotting analysis, aliquots of 50 μg of Raw264.7 cell lysate and 6 μg of phagosomal fractions were separated by SDS–PAGE and then subjected to immunoblotting analysis using anti-Rab5 antibody (1:100 v/v), anti-Rab7 antibody (1:100 v/v), anti-Rab9 (1:100 v/v), anti-Rab14 (1:100 v/v) and anti-Rab22a (1:100 v/v). Band intensity from three independent experiments was quantified by ImageJ (http://rsbweb.nih.gov/ij/).

Thin-section electron microscopy

Phagosomal fractions were isolated at 6 h p.i., fixed with 1% glutaraldehyde in 0.1 M sodium phosphate buffer (pH 7.4) and washed with phosphate buffer. Fixed phagosomal fractions were incubated with 0.1% (w/v) osmium tetroxide. Dehydration was carried out with a series of ethanol washes, followed by treatment with propylene oxide. Samples were embedded in Qetol812 resin (OKEN) according to the manufacturer's protocol. Thin sections were cut with diamond knives and mounted on copper grids. Samples on grids were counter stained with 2% (w/v) uranyl acetate and then observed with a JEM-1220 electron microscope (JEOL).

LysoTracker staining, labeling lysosomal vesicles with fluorescent dextran and immunofluorescence microscopy

For LysoTracker staining, cells were incubated with 300 nM LysoTracker Red DND-99 (Invitrogen) for 30 min before fixation. Stained cells were fixed with 1% paraformaldehyde in PBS for 1 h, washed with PBS and

Uncorrected Proofs